STRUCTURE AND SEDIMENTOLOGY OF THE CAPE FORBIN AREA, SOUTHERN ADELAIDE FOLD-THRUST BELT: IMPLICATIONS FOR REGIONAL TECTONICS.

MARTIN C. FAIRCLOUGH, B.Sc.

Thesis submitted as partial fulfilment of the requirements for the Honours Degree of Bachelor of Science.

November 1992

NATIONAL GRID REFERENCE:

Kingscote (SI-53-16) 1:250 000 sheet

Snug Cove (SI-53-6626-I) & Borda (SI-53-6626-IV) 1:50 000 sheets

THE UNIVERSITY OF ADELAIDE

Department of Geology and Geophysics

COPY 2

Supervisors: P R James, T Flottmann

§1: INTRODUCTION

§1.1: REGIONAL GEOLOGY & OUTLINE OF THE PROBLEMS

The Adelaide Fold Belt (Figure 1) is a major sygmoidal orogen comprising Neoproterozoic to early Palaeozoic sediments folded and metamorphosed during the Cambro-Ordovician Delamerian Orogeny (*Thomson*, 1969). Adelaidean platformal sediments within the southern Adelaide Fold Belt are overlain by Cambrian carbonate/siliciclastics (Normanville Group) and Kanmantoo Group metasediments which crop out in the Fleurieu Arc, structurally trending north-south in the Mt. Lofty Ranges to east-west on Kangaroo Island. The 'flyschoid' Kanmantoo Trough sequence consists largely of turbiditic basinal clastics (*Sprigg & Campana*, 1953) deposited in a rapidly subsiding area adjacent to the basement high of the Gawler Craton (the 'Kangarooian Movements' of *Daily & Milnes*, 1971a).

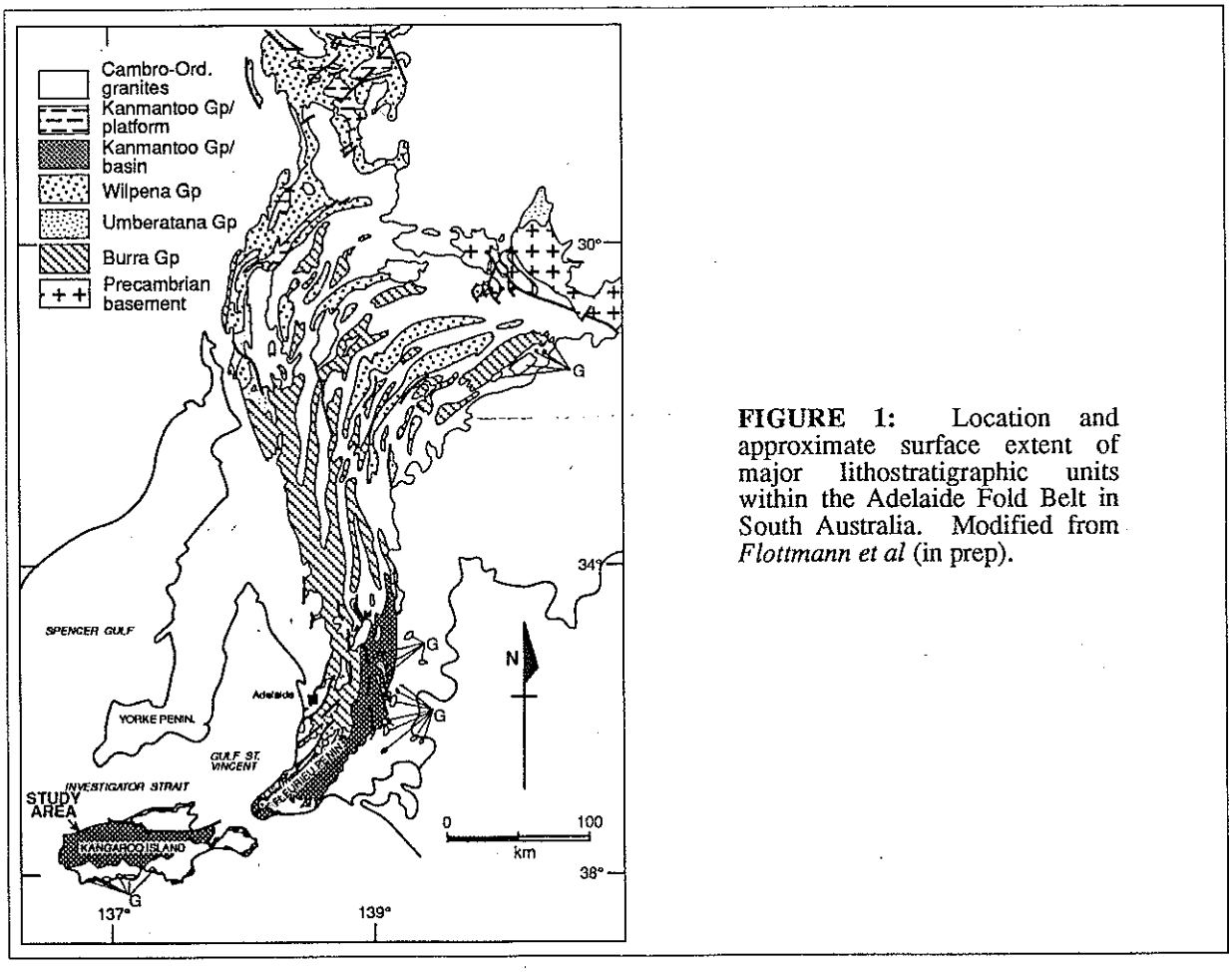

FIGURE 1: Location and approximate surface extent of major lithostratigraphic units within the Adelaide Fold Belt in South Australia. Modified from *Flottmann et al* (in prep).

The body of opinion concerning the regional geology of the southern Adelaide Fold Belt is currently in a state of flux. Previously accepted interpretations under review include;

1). the tectonostratigraphic nature of the Kanmantoo Group: extensional rift-type sedimentation (*Turner* et al, 1992), or a contractional foreland basin setting (*Jenkins & Sandiford*, 1992). If the Kanmantoo Trough was extensional, there is an apparently short period of time (*ca.* 10 m.y.) available for sedimentation (up to 18km; *Gatehouse* et al, 1990), followed by an unusually rapid switch to contraction and deformation. (*Foden* et al, 1992).

2). the seemingly exceptional stratigraphic thickness, commonly faulted contacts with adjacent lithologies and apparently inverted metamorphic facies with respect to the underlying Neoproterozoic sequence has led some workers to speculate that the Kanmantoo metasediments are partially or wholly allochthonous, and may be substantially thickened by as yet unrecognised thrusts (*Jenkins*, 1986; *Steinhardt,* 1989). An inevitable consequence of such gross shortening of the cover sequence is the possibility of thin-skinned deformation. Earlier workers have reported little evidence of a well-developed thrust system, which would be expected in such a tectonic environment. However, *Jenkins* (1990) and *Clarke & Powell* (1989) have recently proposed differing interpretations of the location of thrust traces, whilst Steinhardt (in *James*, 1989a) has suggested the stratigraphic horizons in which such thrusts are likely to occur (Figure 2), and postulated that repetition of Kanmantoo formations has resulted in imbricate thickening and erroneous lithostratigraphic subdivision.

3). the enigmatic nature of the curvature of the fold belt. Various mechanisms have been proposed to account for the arcuate trace of macroscopic fold trends within the orogen, ranging from models involving regional sinistral basement shearing (*Jenkins*, 1990), east-west 'wrench-shearing' (*Clarke & Powell*, 1989), to large-scale fold-interference patterns (*Preiss*, 1987).

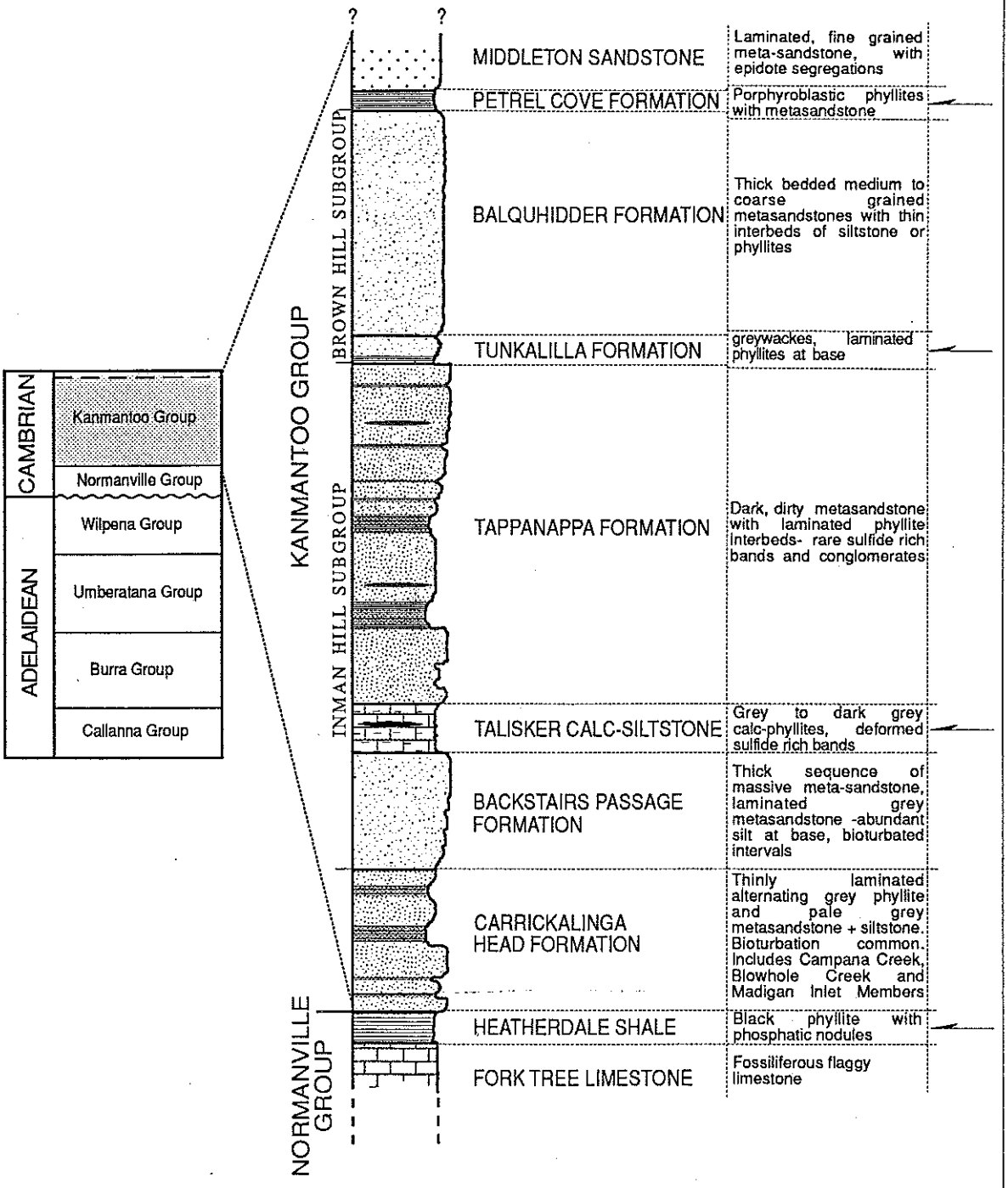

FIGURE 2: Stratigraphic relationships of the southern Adelaide Fold Belt, with indicated horizons in which thrusts may be expected to occur (*Steinhardt*, 1989). Adapted from *Daily & Milnes* (1971a, 1973) and *Preiss* (1987).

§1.2: AIMS AND METHODS OF INVESTIGATION

Recent detailed work (eg. *Johnson*, 1991; *Rogers*, 1991; *Flöttmann* et al, 1992; *Flöttmann & James*, 1992) has attempted to elucidate the structural and stratigraphic relationships within the Kanmantoo Group of the southern Adelaide Fold Belt, and to help solve some of the problems outlined above. The present study is partly a continuation of this program of investigation. Detailed structural investigations were carried out within the chosen 3x9 km field area, situated on the north-west coast of Kangaroo Island (Figure 3). The region was chosen specifically to examine a recently discovered shear zone east of Cape Forbin, and it's possible implications for local and regional geological relationships within the Kanmantoo Group. Geological mapping at a scale of 1:10 000, appropriate strain analysis techniques, and thin-section microstructural analysis were implemented to determine the geometric, kinematic and tectonic evolution of the area. Additional brief investigations were conducted outside of the original study area (eg Harveys Return, Scott Cove; Figure 3) in order to clarify various geological relationships.

The aims of this study also encompass sedimentological and stratigraphic aspects of the Cape Forbin area. Such studies are, in part, intended to provide some understanding of the (disputed) depositional environments of the Kanmantoo Group. Consequently, detailed sedimentological examinations are intended to provide important information upon the tectonostratigraphic evolution of the Kanmantoo Trough. Furthermore, it is intended that the present study will be a useful adjunct to regional geological mapping presently being conducted by geologists of the S.A. Department of Mines & Energy, in preparation for the revised version of the KINGSCOTE 1:250 000 sheet. To this end, an attempt has been made to correlate the previously 'undifferentiated' lithologies within the area with known Kanmantoo Group formations elsewhere in the southern Adelaide Fold Belt. This was achieved by a detailed study of all available stratigraphic information concerning the Kanmantoo Group, examination of the type-section on the south coast of the Fleurieu Peninsula, and consideration of local structural complexities between areas of known stratigraphy and the Cape Forbin region.

§1.4: PREVIOUS INVESTIGATIONS

Isolation, difficult access and paucity of non-coastal outcrop has ensured that the majority of early geological work related to Kangaroo Island has been of a regional and/or preliminary nature (eg. *Bauer*, 1958). Consequently, with several notable exceptions, detailed investigations are lacking, and this is particularly true for the area under consideration. *Sprigg* et al (1954) presented the first comprehensive attempt at a regional geological map, but much of the area mapped as Precambrian (including the Cape Forbin region) is now considered to be Cambrian Kanmantoo Group by the majority of recent workers (*Belperio & Flint*, 1992a).

Regional studies by *Mancktelow* (1979, 1990) showed that the bedrock structure of the Island consisted of a series of east-west trending macroscopic folds, including the West Bay syncline situated along, and sub-parallel to, the north-west coast. *Mancktelow* (1979) and *Offler & Fleming* (1968) established the approximate location of regional metamorphic isograds by noting the presence of characteristic mineral assemblages. Both considered the Cape Forbin area to be within the biotite grade zone. Furthermore, these workers noted the presence of three, and possibly four, distinct deformation events within the southern Adelaide Fold Belt, of which the macroscopic folds (including the West Bay syncline) were interpreted to be D_1 features. In a more detailed study concerned with the West Bay area (Figure 3), *Flint & Grady* (1979) also reported three deformations on the basis of a series of purportedly discrete fold generations (although no crosscutting fabrics were reported).

Stratigraphic investigations have been largely restricted to Dudley Peninsula (*Daily & Milnes*, 1971b, 1972) to the east, where individual units have been correlated with their equivalent type-sections on the Fleurieu Peninsula (*Daily* et al, 1979). Elsewhere on Kangaroo Island, including the present study area, the Kanmantoo Group has not previously been subdivided with any degree of confidence (*Gravestock*, in prep.).

§2: SEDIMENTOLOGY AND STRATIGRAPHY

§2.1: SEDIMENTOLOGY

Traditionally the Kanmantoo Group has been regarded as having deeper water 'flysch-like' affinities (*Sprigg & Campana*, 1953; *Mancktelow*, 1979; *Boord*, 1985; *Gatehouse* et al, 1990), associated with rapid deposition within a deeply subsiding, fault-bound trough. However *Daily & Milnes* (1971a, 1973), in their stratigraphic subdivision of the group into eight formations (Figure 2), presented a modified interpretation of much of the sequence. Instead, they (*op cit*) emphasised significant influence by traction-currents indicating a shelfal environment. Consequently different formations within the Kanmantoo Group have been attributed variously to continental shelf, continental slope and ocean basin depositional environments (*Belperio & Flint,* 1992a).

Dark to pale grey metasandstones within the study area are generally typical of the Kanmantoo Group. In detail however, there are subtle lithological variations which can be discerned via a traverse across strike. Lithologies toward the west of the area are dominated by interbedded strongly laminated psammites/pelites separated by massive, pale-grey quartzites (referred to subsequently as 'Sequence One' deposits; Plate 1b). Stratigraphically up-section to the east, the laminated units thin and become more faintly laminated, whilst thick, 'dirty' metasandstones with occasional fine-grain sandstone and phyllitic partings begin to dominate the outcrop ('Sequence Two' deposits; Plate 1c). It should be emphasised that this transition is barely perceptible and irregular (Sequence One outcrops occur within the Sequence Two area and vise versa), but nevertheless has important implications for sedimentological interpretations and the styles of deformation encountered in the respective areas (see §3.1).

The youngest equivalents of the Kanmantoo Group within the area crop out to the west of Cape Forbin, where Sequence One deposits are exposed in high coastal cliffs above a small wave-cut platform. The rocks in this vicinity essentially consist of laminated sandstones with characteristic biotite-rich and quartz-rich layers, and extend at least as far west as Scott Cove.

The quartz-biotite laminated units characteristic of Sequence One deposits are intercalated with massive, clean quartzite beds varying in thickness from individual laminae up to 1-2 metres. These latter beds also occasionally show faint planar biotite concentrations, and commonly the transition from massive quartzite to overlying laminated unit is gradational. In contrast the contact between the massive quartzite and the *underlying* laminated horizon is generally sharp or convolute, and commonly clearly an erosional surface (Plate 1d). Within the laminated units, the quartz-rich layers are generally thicker than adjacent biotite-rich layers; the latter are rarely greater than 1 cm. in thickness.

Talbot & Hobbs (1968) and *Daily & Milnes* (1973) report similarly prominent laminations elsewhere in the Kanmantoo Group, in the Petrel Cove and Tapanappa Formations respectively. These workers attribute these 'stripy layers' to post-lithification metamorphic differentiation or alteration processes adjacent to fractures. Clearly, however, the 'black and white' layering evident in the rocks of northwest Kangaroo Island (particularly at Harveys Return; see fig. 24 in *Daily* et al, 1979) is a result of primary sedimentary processes: 1) biotite concentrations define a variety of sedimentary structures (Plate 1e); 2) there is no indication of a pervasive layer-parallel fabric (in the sense of *Maltman*, 1981) in fact, the regional slaty cleavage/schistosity consistently transects the biotite-quartzite banding at a shallow angle; 3) the diffuse and 'wispy' nature largely characteristic of metamorphic banding is essentially absent.

The remarkably strong sedimentary laminations are interpreted here to result from reworking of relatively homogeneous beds via traction processes and deposition of fines from a suspended load. Such hydraulic sorting processes are suggested to have winnowed clay/biotite from mica-rich sands, with subsequent redeposition as discrete clay/biotite laminae. The strong contrast in hydraulic behaviour between coarse sand grains and biotite flakes enabled different mineral loads to be deposited separately. The extent to which differentiation occured was variable, depending upon complex interplay between fluctuations in depositional flow regime and rate of sedimentary supply. Massive grey quartzites represent episodes of relatively inefficient sorting, probably during periods of more constant influx and deposition. This

interpretation is supported by the observation that the massive units are frequently erosive into laminated units, and 'ball-and-pillow' structures are largely represented by massive sands enclosed by laminations (rarely visa versa). As such, they were probably laid down rapidly as debris flows (see *Gatehouse* et al, 1990). This is consistent with other indications of rapid deposition (Plate 1f), such as a complete lack of bioturbation, carbonate deposition, and liquefaction structures, as defined by *Owen* (1987).

More strongly laminated units are presumably indicative of periods when the effects of reworking exceeded the effects of rapid deposition. The frequently gradual transition from massive to crossbedded rocks (Plate 1e) supports this concept, in that it represents the effects of diminishing reworking of the sedimentary unit with depth. Lithologies transitional between Sequence One and Sequence Two types attest to the variable efficiency of sediment reworking processes. The ubiqitous sedimentary evidence for reworking of relatively immature sands into well-sorted, laminated and crossbedded deposits, points towards a relatively shallow-water, moderate to high energy depositional environment. Indeed, at some localities reworking progressed to the extent of producing large-scale foreset beds of clean quartz sands, similar to those derived from sand-waves within tide-dominated environments (*Reading*, 1986). However, there is no indication of temporary emergence, nor is there any definitive evidence of high energy storm activity (eg hummocky cross-stratification) indicating a shore-type environment. Presumably the prime physical processes were offshore oceanic or tidal currents.

In contrast the *relatively* texturally and mineralogically immature (although the term 'greywacke' is perhaps too extreme) Sequence Two deposits may exhibit the least reworking of all the lithologies present, possibly related to a slightly deeper water environment. They show little evidence of shallow water modification: the only sedimentary structures observed are poorly defined sedimentary slump folds. However, Sequence One sediments comprise most of the rocks in the study area. Consequently, the sedimentary environment concluded is one of shallow-water (<50m; cf.*Fenton & Wilson*, 1985) sand sheets reworked from rapidly laid down debris flow deposits. Certainly a *deep-water* turbidite scenario is not indicated by this study.

§2.2: STRATIGRAPHIC RELATIONSHIPS

Stratigraphic correlation within the Kanmantoo Group is subjective and fraught with uncertainty, particularly due to the lithological homogeneity of the sequence. Indeed Steinhardt (in *James*, 1989a) tentatively asserts that one possible reason for the similarity between the constituent formations is that they *are* the same. The implication is that gross thrust repetition invalidates the accepted stratigraphic subdivision of the entire group. Nevertheless, whilst regional tectonic thickening may be important, *Johnson* (1991) and *Rogers* (1991) demonstrated that the stratigraphy established by *Daily & Milnes* (1971a, 1973) was locally viable. Consequently the scheme of Figure 2 is utilised here.

Examination of the Kanmantoo Group type-section and all relevant literature suggests that the Cape Forbin sequence is most likely to be an equivalent of the Tapanappa Formation. The dark quartzite with phyllitic partings described by *Daily & Milnes* (1971a, 1973) is very similar to the Sequence Two deposits within the study area. These, in turn, are virtually identical to relatively deep-water lithologies to the west assigned to the Tapanappa Formation by *Flint* (1978). To the east, drilling investigations suggest that the Dewrang geophysical anomaly is hosted by Tapanappa Formation type sandstone (*McCallum*, 1991, p. 29). Conversely, the shallow-water deposits of Sequence One are strikingly similar to Tapanappa equivalents on Dudley Peninsula (*Daily* et al, 1979), particularly at Cape Coutts, and Inman Hill Subgroup laminated psammites and pelites at Harveys Return (*Major & Vitols*, 1973). *Mancktelow* (1979) considered that local lithostratigraphic units were correlatable with the Middleton Sandstone. Clearly, however, there are no local indications of the epidote-rich segregations considered to be diagnostic of the Middleton Sandstone, and therefore the resemblance is considered to be superficial only. *Mancktelow* (1979) reports the presence of two distinct lithofacies of the Tapanappa Formation on Fleurieu Peninsula, which may correspond to the two different sequences outlined in this study.

§2.3: REGIONAL IMPLICATIONS

The sedimentary sequence within the study area is conformable from east to west, and apparently as far west as Cape Borda (*Major & Vitols*, 1973). Even allowing for small scale tectonic folding, this represents a thick package of rapidly deposited strata. Such a feature requires a consistently emergent source region adjacent to an actively subsiding basin (the 'Cassinian Uplift' and 'Waitpingan Subsidence' respectively of *Thomson*, 1969), as is the case for much of the Kanmantoo Group. Most workers attribute the provenance of the entire group to emergent landmasses to the north of the Kanmantoo Trough (eg *Daily & Milnes*, 1973; *Daily* et al, 1980). Implicit in all such investigations is that such tectonic movements were of an extensional nature. *Jenkins* (1990), however, has suggested that the Kanmantoo Group is partly syn-orogenic. This raises the possibility that the evolution of the Kanmantoo Trough records a significant component of contractional tectonism, with deposition in a foreland basin marginal to a source converging from the south-east (cf. *Jenkins & Sandiford*, 1992).

Palaeocurrent data within the study area is complicated by shallow-water current reworking, presumably reflecting the geometry of the Cambrian shoreline. However, it can be demonstrated that a significant component of turbidity current fabric is still preserved (Plate 2a), occasionally with clear indications of mass-flow directions (Plate 1d). Furthermore, in relatively undeformed areas, syndepositional deformation structures display slight asymmetries in an opposite sense to tectonic features, but consistent with the aforementioned mass-flow current directions (Plate 1f). Whilst it was not possible to unequivocally separate many palaeocurrent indicators into 'shallow-water' and 'turbiditic' signatures, the cumulative data (Figure 8) reveals little distinction between the respective types. Both mass-flow influx and shallow-water progradation originate from the west and north-west, with most definitive turbidite fabrics accounting for the latter direction. In addition to this data from probable Tapanappa equivalents, equivalent mass-flow palaeocurrent data elsewhere in the Kanmantoo Group indicates a similar provenance area (eg *Flint*, 1974, 1978; *Mancktelow*, 1979; *Boord*, 1985). Such evidence is not consistent with a contractional source region encroaching from the south or south-east.

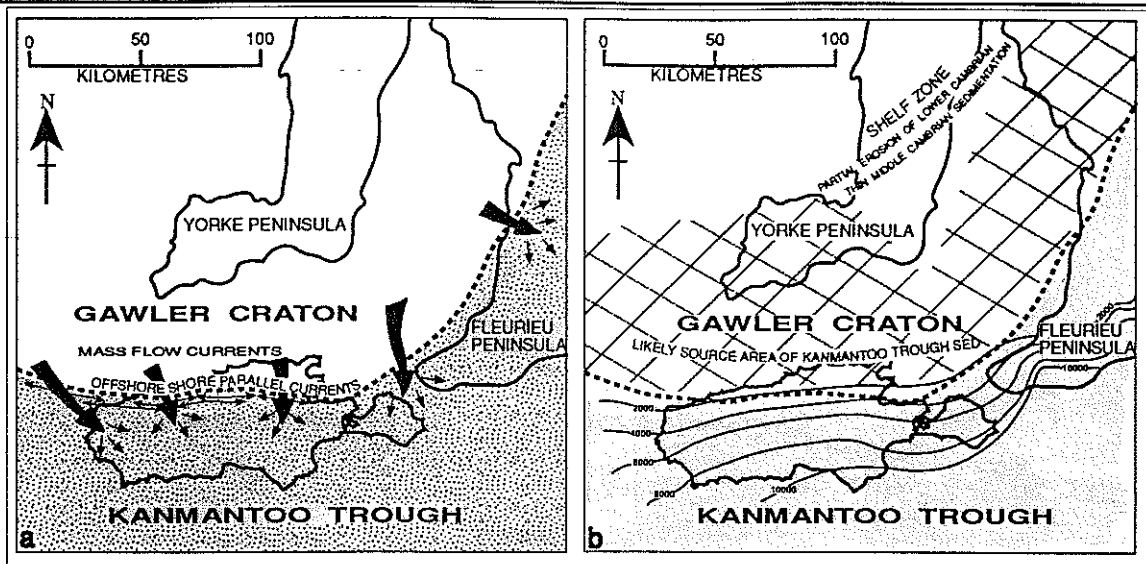

FIGURE 4: Palaeogeography of the Kanmantoo Group. **a.** Interpreted palaeocurrent directions and marine influences of Kanmantoo sediments marginal to the Gawler Craton. **b.** Inferred provenance of the Kanmantoo Group and approximate sedimentary thicknesses (in metres) from regional mapping. Data compiled from this study, *Thomson*, 1969, 1975; *Flint*, 1978.

Whilst there is much evidence to indicate an extensional terrain for the currently exposed levels of the Kanmantoo Group [not the least of which is stratigraphic thickening across syndepositional normal faults (*Rogers*, 1991)], there are several pertinent points which concern the continued tectonostratigraphic evolution of the trough. According to *Jenkins* (1990), although the lower segments of the sequence (specifically the Carrickalinga Head Formation and the underlying Normanville Group) are intimitely associated with the Truro Volcanics, indicating lithospheric attenuation via extension, there is "a complete alternation of sediment provenance and basin geometry" in the transition from the lower Kanmantoo Group and the supposedly younger 'molassic apron' of the upper Kangaroo Island Group. The relationship between the upper levels of the Kanmantoo Group and basin geometry is, however, unknown, because the "upper boundary of the group remains undefined" (*Sprigg & Campana*, 1953). Evidence from granite intrusions suggest that at least 10km of sedimentary pile existed *above* the Middleton Sandstone. If the transition from extensional to contractional deposition occured, it is most likely to be represented within the 'missing' higher sections; not within the Tapanappa Formation of Cape Forbin. Interestingly, *Daily* et al (1979) speculate that Kanmantoo metasediments on the south coast of Kangaroo Island may be stratigraphically higher than the Middleton Sandstone, and therefore these may be the syn-orogenic strata of *Jenkins* (1990).

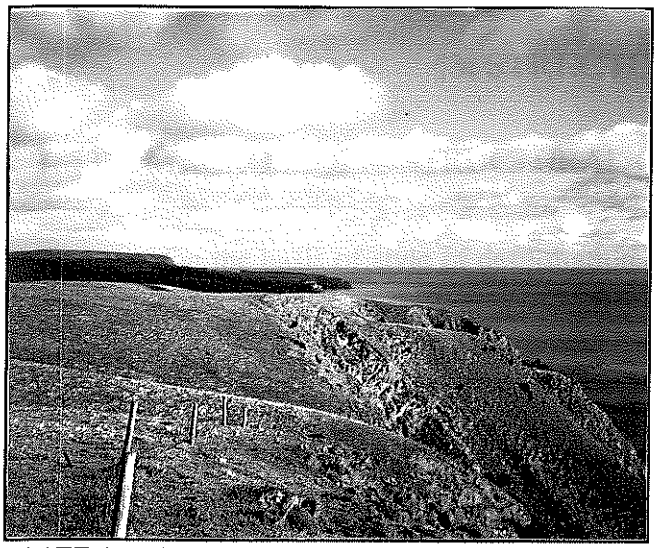

PLATE 1a: View of study area looking west towards Cape Forbin. Kangaroo Gully is in the foreground, Cape Torrens is in the distance. [Snug Cove; 662478].

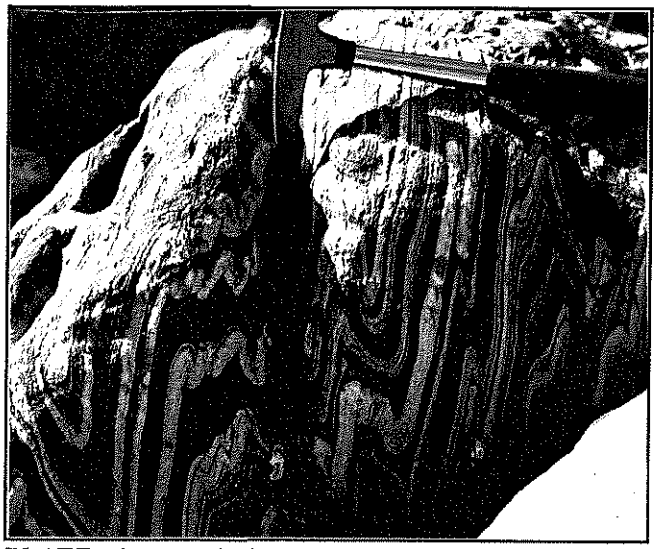

PLATE 1b: Typical cross-laminated Sequence One psammite and psammite/pelite multilayer. Looking south, width of view = 40 cm. [Borda; 573451].

PLATE 1c: Typical massive to poorly bedded 'greywacke' of Sequence Two deposits. Looking east, width of view = 1m [Snug Cove; 665474].

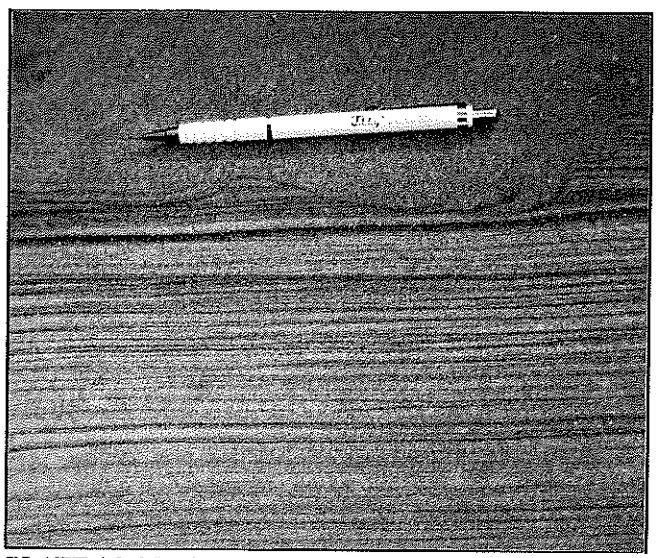

PLATE 1d: Massive, poorly sorted T_A 'greywacke' erosive into well sorted psammite/pelite multilayer. Looking south, pencil = 14 cm. [Snug Cove; 609464].

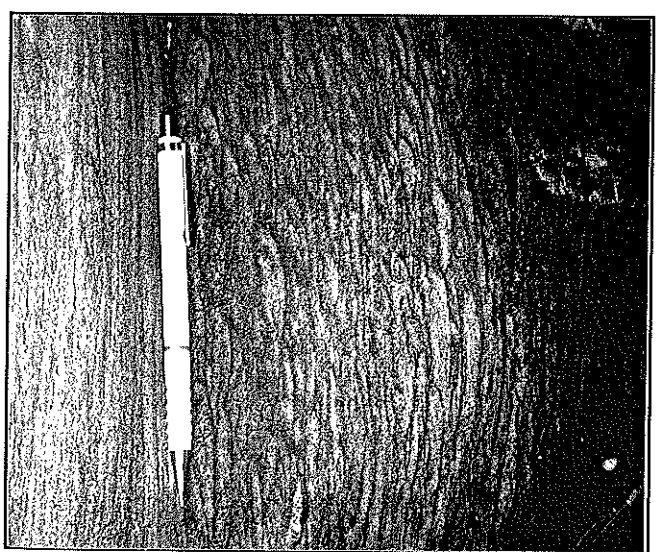

PLATE 1e: Trough cross-laminations defined by biotite concentrations. Looking south, width of view = 50 cm. [Snug Cove; 609464].

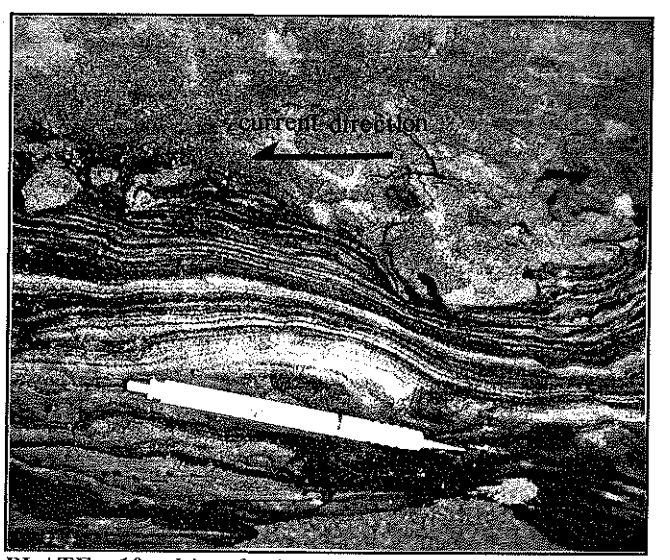

PLATE 1f: Liquefaction structure indicating rapid deposition of 'greywacke' onto unlithified multilayer. Looking south, pencil = 14 cm. [Snug Cove; 593454].

§3: STRUCTURAL GEOLOGY

§3.1: MACROSCOPIC STRUCTURAL GEOMETRY

On the basis of style of deformation and strain intensity, the Cape Forbin area can be conveniently subdivided into two major structural domains. The high strain Snug Cove Shear Zone to the north is transitional into the structurally overlying country rock of the Back Valley Homoclinal Zone extending to the south and west (Figure 5). Both domains dip moderately to the south and occur on the right-way-up limb of the regional West Bay Syncline (*Mancktelow*, 1979). The east-west strike of the shear zone is sub-parallel to regional bedding trends, but is locally slightly discordant (<20°) due to the closure of the major syncline to the west. The relationship between the present study area and regional structures as mapped by previous workers is illustrated in Figure 6. A tentative and schematic re-interpretation of regional sub-surface structure, taking into account the Snug Cove Shear Zone, is also presented.

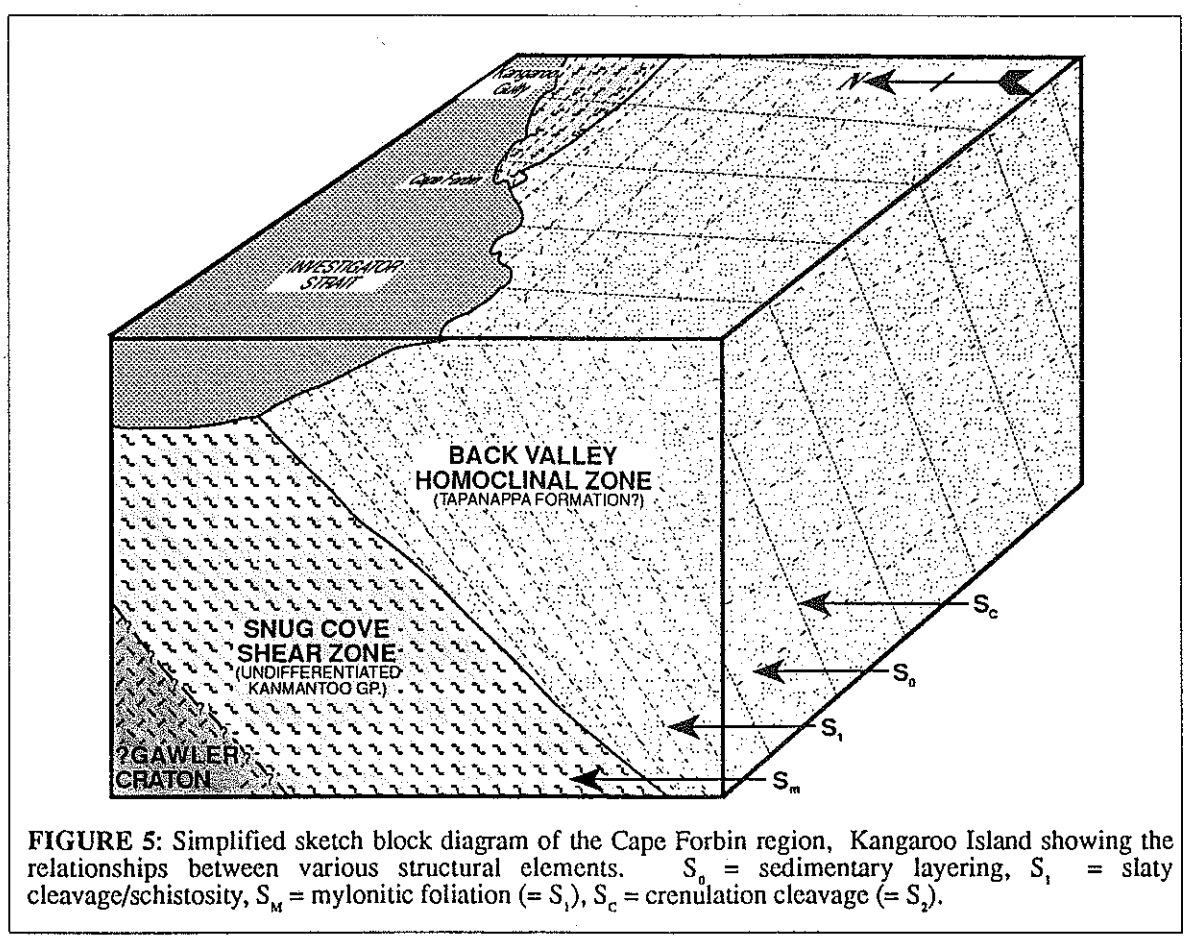

FIGURE 5: Simplified sketch block diagram of the Cape Forbin region, Kangaroo Island showing the relationships between various structural elements. S_0 = sedimentary layering, S_1 = slaty cleavage/schistosity, S_M = mylonitic foliation (= S_1), S_C = crenulation cleavage (= S_2).

§3.1.1: Metamorphic And Structural Fabrics

A single prominent metamorphic fabric defines the main foliation S_1 and occurs as an east-west striking slaty cleavage, schistosity or mylonitic foliation (S_{1M}) dipping steeply to the south. The foliation is largely defined by preferred orientation and growth of micas (mainly biotite) and is therefore more pronounced in pelitic Sequence One deposits (particularly within minor folds) where it is strongly refracted across bedding. In the more massive Sequence Two deposits S_1 is non-existant to poorly-developed and occurs as a weak spaced cleavage.

A traverse from south to north shows a gradual increase in the intensity of the S_1 foliation independent of lithological variation, and is associated with an increase in minor faulting and folding. A relatively abrupt, *but still gradual,* change separates the shear zone from the country rock where the foliation aquires an anastomosing mylonitic character (§3.3) and a moderately to strongly developed mineral lineation. The boundary is mapped as the region in which bedding is largely transposed and/or indistinguishable due to the mylonitic foliation. The lineation is parallel to the elongation direction of stretched porphyroblasts (used to estimate finite strain ratios in §3.2.3), elongate quartz rods and boudins within lithological layering. It is therefore a stretching lineation (L_1) representing the maximum axis of the local finite strain ellipsoid (X) within the foliation plane XY (where X>Y>Z) and delineating the tectonic transport direction (*Wood*, 1974). L_1 is largely a near down-dip lineation, plunging on average towards 170°. The exception to this remarkably consistent feature is a small area in the vicinity of Cape Forbin proper, where L_1 is oblique-dip and pitches ~40-50 east within S_1.

Within the Back Valley Homoclinal Zone a bedding/cleavage intersection lineation (L_1^0) is also present, which is best developed marginal to the Snug Cove Shear Zone where it defines isoclinal fold axes and is sub-parallel to L_1. Elsewhere in the study area the intersection lineation and fold axes strike east-west. All of the above fabrics are attributed to a single deformation (D_1) of variable intensity; no crosscutting relationships were observed between, for example, the regional slaty cleavage and the local mylonitic foliation. It seems likely that the local S_1 is equivalent to the regional foliation which is axial planar to the D_1 West Bay syncline

(*Mancktelow*, 1979,1990). An isolated and weak later post-D_1 crenulation cleavage (S_2) was encountered in a small number of outcrops within rare D_2 kink folds. This foliation is defined by alignment of biotite and muscovite and is sub-vertical to steeply east dipping. S_2 is, at best, weakly developed and was mainly observed crenulating the most intensely developed S_1 fabric, the mylonitic foliation. The associated D_2 fold axes and intersection lineations (mainly L_2^1) dip moderately to the south. The relationship between the local S_2 and regional foliations is unclear.

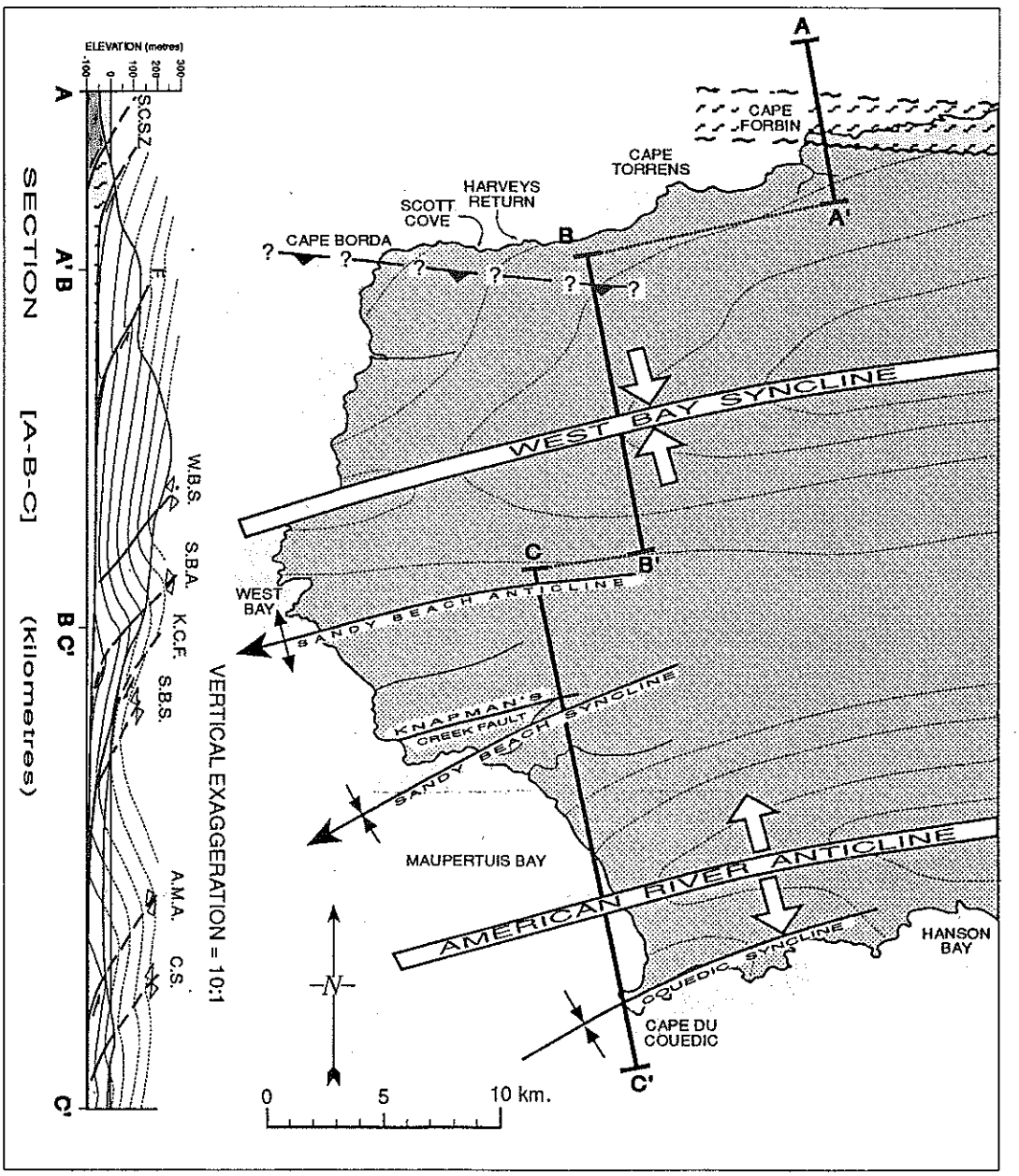

FIGURE 6: Regional structural geology and interpretive cross-section of western Kangaroo Island. No attempt has been made to balance the section due to a lack of stratigraphic control. Synthesis compiled from numerous sources, including this study; *Sprigg et al*, 1954; *Thomson*, 1969, 1975; *Major & Vitols*, 1973; *Mancktelow*, 1979, 1990; *SADME*, 1989; *Belperio & Flint*, 1992b, and *Van der Stelt et al*, 1992.

§3.1.2: Faulting

Small-scale brittle faulting is common throughout the study area. High angle reverse faults, striking sub-parallel to the regional S_1 foliation, displace bedding by no more than 1-2 metres (commonly only several centimetres). Although some conjugate faults were observed, by and large steeply dipping faults parallel to S_1 are dominant. Displacement on the latter set of faults commonly occurs along south-dipping quartz veins which are axial planar to minor folds. Bedding offsets and 'stepped' slickensides on quartz vein surfaces indicate reverse motion to the north. The upper boundary of the Cape Forbin Sub-domain is interpreted to be one of these faults (the only segment of the shear zone boundary that is faulted). Although the sense of movement could not be determined directly, it is assumed that it is consistent with similar small-scale faults. At the interface between psammites and less competent phyllites or pelites, brittle faulting often gives way to layer-parallel ductile shearing (again showing top-to-the-north sense of movement; Plate 2b), particularly in higher strain areas to the north.. Where larger portions of east-west striking faults are exposed, fault traces were observed to be listric in form, curving into low-angle thrust-faults (Plate 2c).

In addition to south-dipping contractional faults, the Snug Cove Shear Zone is also dissected by numerous small-scale strike-slip faults, again mostly displaying only one or two metres displacement at most. These faults are sub-vertical and strike approximately north-south. Such faults are confined to areas of highly sheared rocks and are consequently interpreted as a result of differential transport in the direction of shearing (north).

A third set of rare faults is associated with the D_2 folds and fabric. Second generation kink folds grade into high-angle reverse faults, or are located immediately adjacent to them. In some cases a significant component of oblique-slip movement was apparent in these D_2 faults, making them difficult to distinguish from D_1 strike-slip faults. One plausible explanation for such a feature is that D_2 faults were preferentially initiated at, and reactivated some, D_1 faults.

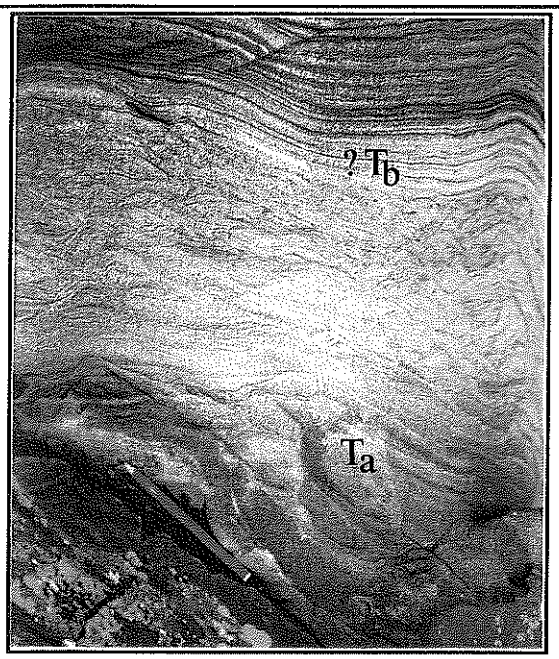

PLATE 2a: Partial Bouma sequence, including basal greywacke (T_A) and laminated ?T_B horizon, Harveys Return. [Borda; 481426].

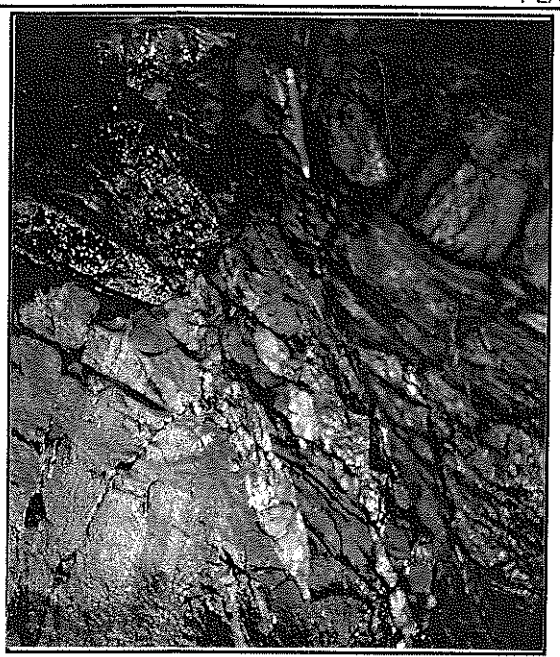

PLATE 2b: Layer-parallel ductile shearing consistent with top-to-the-north simple shear. Looking east. Note pencil for scale. [Snug Cove 665476]

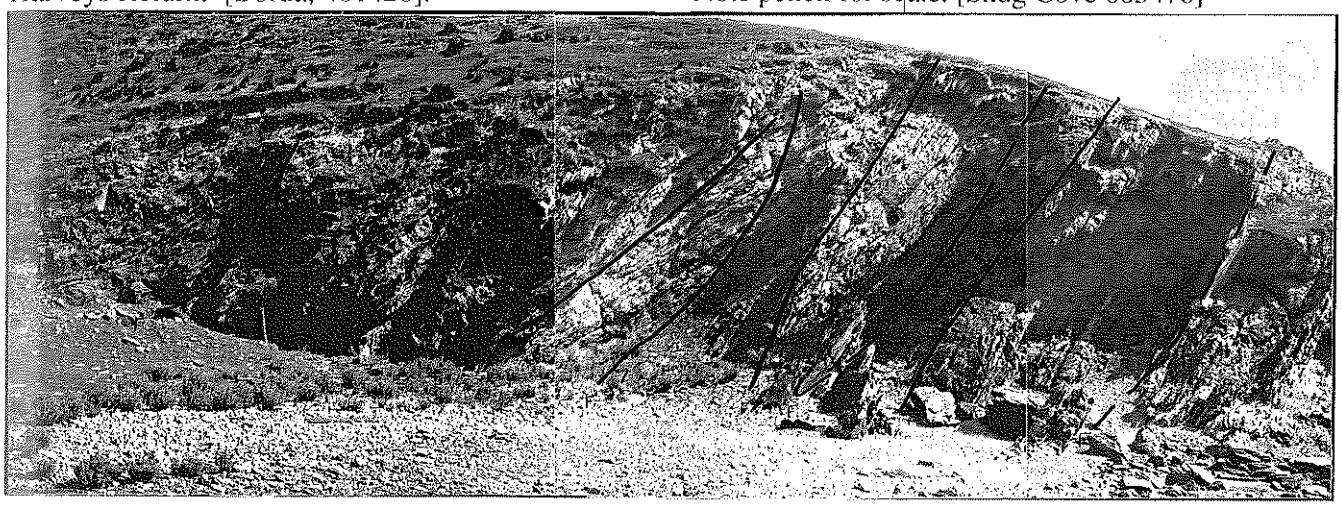

PLATE 2c: Listric reverse and thrust faults, Wreck Gully. Looking west. Note figure for scale. [Snug Cove 665482].

PLATE 2e: Buckling of sub-vertical quartz vein by shortening across S_1. Width of view ≈ 50 cm. View looking east. [Snug Cove 635477].

FIGURE 2f: Overturned, north-verging fold with intense, moderately dipping axial planar cleavage. Width of view ≈ 40 cm. Looking east. [Borda 579452].

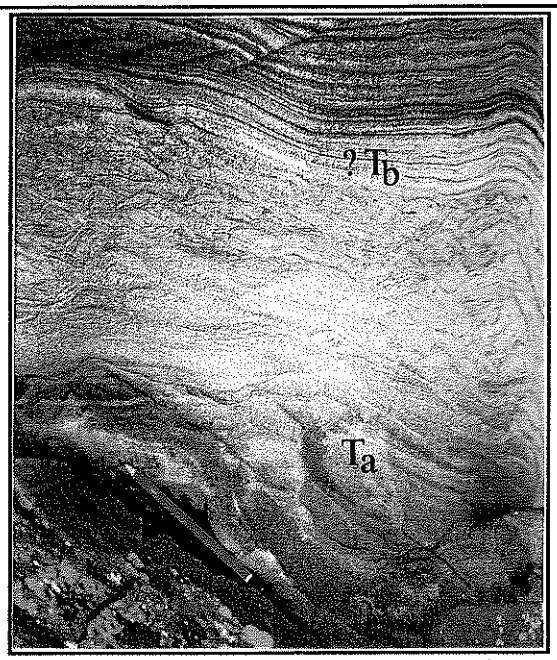

PLATE 2a: Partial Bouma sequence, including basal greywacke (T_A) and laminated $?T_B$ horizon, Harveys Return. [Borda; 481426].

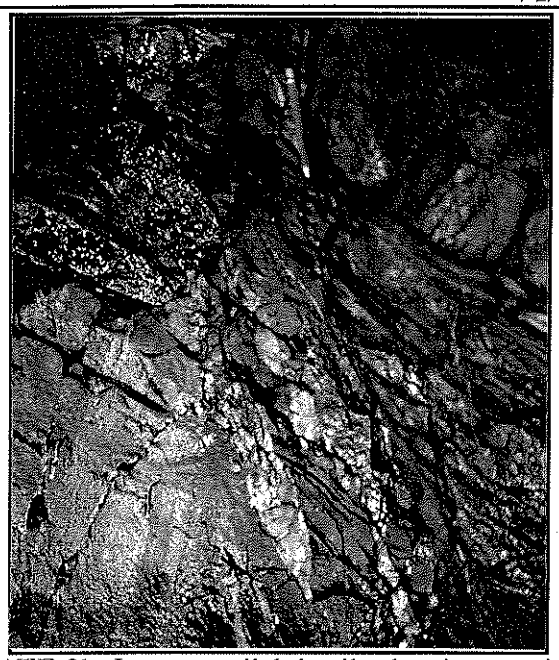

PLATE 2b: Layer-parallel ductile shearing consistent with top-to-the-north simple shear. Looking east. Note pencil for scale. [Snug Cove 665476]

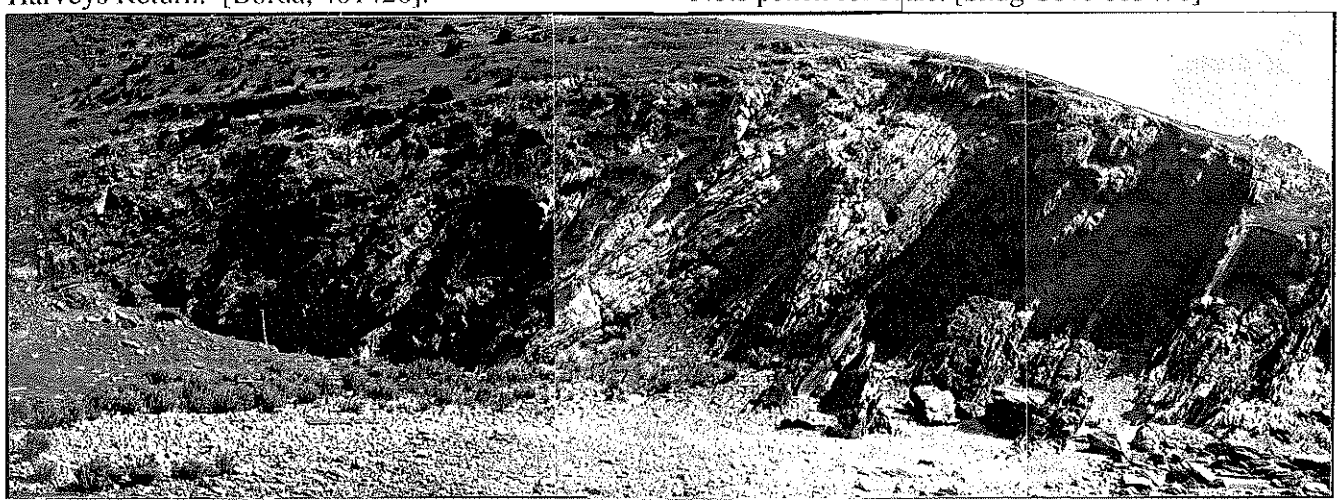

PLATE 2c: Listric reverse and thrust faults, Wreck Gully. Looking west. Note figure for scale. [Snug Cove 665482].

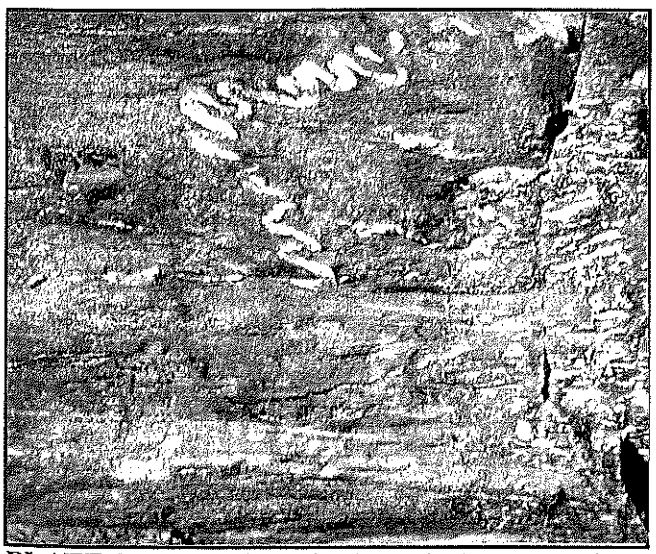

PLATE 2e: Buckling of sub-vertical quartz vein by shortening across S_1. Width of view ≈ 50 cm. View looking east. [Snug Cove 635477].

FIGURE 2f: Overturned, north-verging fold with intense, moderately dipping axial planar cleavage. Width of view ≈ 40 cm. Looking east. [Borda 579452].

§3.1.3: Quartz Veining

Perhaps one of the most notable structural features encountered in the Cape Forbin region are the ubiquitous quartz veins, which reflect the strain variation across the study area. Within the Back Valley Homoclinal Zone these veins were observed to be relatively undeformed planar features sub-parallel to S_1. In many instances folding was intimately associated with individual veins. Quartz veins intruded axial planar to many folds (cf. *James* 1989b) and show no definitive features associated with extension normal to the axial planar cleavage (eg. fibrous quartz, median lines, etc). This vein array is thus attributed to elevated pore pressures leading to hydraulic fracturing along planes of weakness (ie cleavage anisotropies), a feature commonly encountered in areas associated with shear zones and shear strain localization (eg *Flöttmann et al*, 1992).

Although the great majority of vein formation is clearly a consequence of the nature of fold axial planar cleavages, on rare occasions complex fold patterns are observed which indicate a normal sense of bedding offset along veins. Intuitively such evidence indicates that the some quartz veins have played a role in controlling fold morphology. This feature was mostly confined to poorly laminated Sequence Two deposits, and thus is difficult to discern and document. Such apparent offsets are the *only* kinematic criteria in the study area which indicate north-south extension and thus appear anomalous. *Hudleston* (1989) describes similar folds and offset patterns in glaciers which give sense of shear opposite to the known regional sense. Available experimental evidence (*Hudleston*, 1989) suggests that such folding is a consequence of strain perturbation around a rotating rigid quartz vein. *Hudleston* (1989) has demonstrated that complex fold patterns can form as a consequence of the rotation of originally dilational veins initiated at approximately 45° to regional shear planes. Subsequent rotation and closure of the veins causes pre-existing layers cut by the fracture to become folded (Figure 6b). Because the vein material is stiffer than the host metasandstones, upon rotation it will buckle, unfold and subsequently boudinage, depending upon simple shear strain intensity. Some evidence of such a process operating is the presence of a limited number of sub-vertical to

steeply north dipping veins, all of which are buckled across the foliation plane (Plate 2e), in close proximity to south-dipping axial planar quartz veins described earlier. There is therefore some qualitative evidence, from quartz veins, of a significant rotational strain component (ie simple shear) within the Back Valley Homoclinal Zone (*cf.* $\gamma \approx 2$, Figure 6b). Such evidence is in agreement with results obtained from tightening and rotation of angular folds (§3.2.1).

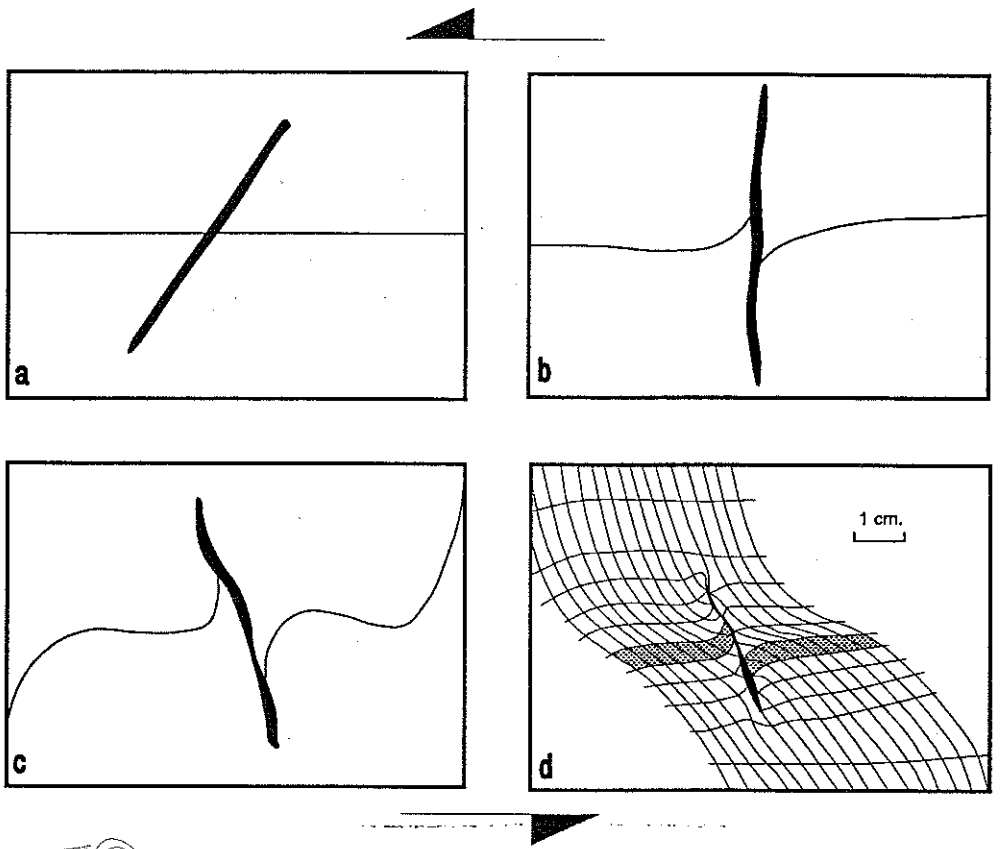

FIGURE 14: Development of 'hook-folds' shown by line drawings of Plasticine blocks used in experiments to show fold production adjacent to fractures. (**a**): Initial state with markers shown drawn parallel to shear zone boundaries and a cut at 45 degrees. (**b**): After left-lateral shear strain of about $\gamma \approx 1$. (**c**): After shear strain of about $\gamma \approx 2$. The ends of the blocks are not shown. (**d**): Line drawing of photograph showing deformation around a deformed vein (black). The grid was originally rectangular, with square elements. One row is stippled to show offset. Modified from *Hudleston*, 1989.

Quartz veins within the Snug Cove Shear Zone are highly deformed, exhibiting extreme boudinaging within the XZ-plane and in many cases defining intrafolial folds in both XZ and YZ-planes. In addition, several examples of sigmoidal en echelon tension gashes were observed (§3.3). These features reflect the high simple shear strain localisation evident within the shear zone, attesting to the excellent strain indicators presented by these quartz veins.

§3.2: THE BACK VALLEY HOMOCLINAL ZONE

The Back Valley Homoclinal Zone, named after a local topographic feature, forms the hangingwall block to the south of the Snug Cove Shear Zone. Although essentially homoclinal at map scale, minor folding is present at outcrop and microstructural level. In general sedimentary bedding (S_0) dips moderately to the south or south-east (Figure 8) and is transected by a slightly steeper dipping slaty cleavage or schistosity (S_1) striking east-west (Figure 9). The cleavage development varies locally in relation to lithology and position within minor folds, but is more intensely developed proximal to the shear zone (ie. to the north). Consistent bedding/cleavage relationships in conjunction with abundant younging criteria are consistent with a structural position on the right-way-up limb of a major fold. Stereographic analysis of intersection lineations (L_1^0) reveals the regional synclinal fold axis to be sub-horizontal and striking approximately east-west (~ 093°; Fig. 10).

Structural variation within the area is generally not dramatic, with most variation manifested within discrete folds or fold pairs separated by large distances of homoclinally dipping strata. This mode of localised folding is common in areas of highly anisotropic rocks (*Price & Cosgrove*, 1990). Consequently, deformational features are most apparent within the psammites and psammite/pelite multilayers of Sequence One deposits mostly to the west of the study area. Although only few folds were observed within this zone, largely concentrated adjacent to the shear zone, the variation evident in these rare folds is nevertheless significant. The effects observed can be categorized into three types; 1) the gradual tightening of folds proximal to the shear zone accompanied by a slight decrease in cleavage plane dip, 2) the development of fold axes oblique to the regional trend, and 3) the lithologically controlled variation in fold styles. Although not mutually exclusive, for simplicity these three factors are considered separately.

MAP ONE

GEOLOGY OF THE SNUG COVE-CAPE FORBIN AREA, KANGAROO ISLAND

GEOGRAPHICAL FEATURES AND MAJOR GEOLOGICAL ELEMENTS

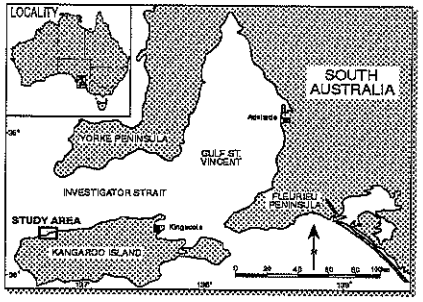

KEY TO MAP ONE

- RIVERS/CREEKS
- UNSEALED ROAD/TRACK
- TECTONIC BOUNDARY (observed/inferred)
- GEOGRAPHIC GRID LINES (Snug cove and Borda 1:50 000 Topographic Sheets)
- LITHOLOGICAL BOUNDARY (observed/inferred)

INVESTIGATOR STRAIT

CAPE FORBIN SUB-DOMAIN

'Eagles Nest'

Cape Forbin

SNUG COVE SHEAR ZONE

Covenys Gully

Whale Gully

Kangaroo Gully

Wreck Gully

BACK VALLEY SUB-DOMAIN TWO

'Snug Cove'

BACK VALLEY SUB-DOMAIN ONE

Snug Cove Road

'The Blowhole'

De Mole River

APPROXIMATE LIMIT OF OUTCROP

BACK VALLEY HOMOCLINAL ZONE

Investigator Way

SCALE

KILOMETRES 0 1 2

G.N.

M.N.

45

44

57 58 59 60 61 62 63 64 65 66

MAP TWO

GEOLOGY OF THE SNUG COVE-CAPE FORBIN AREA, KANGAROO ISLAND

SELECTED BEDDING, YOUNGING & PALAEOCURRENT DIRECTIONS

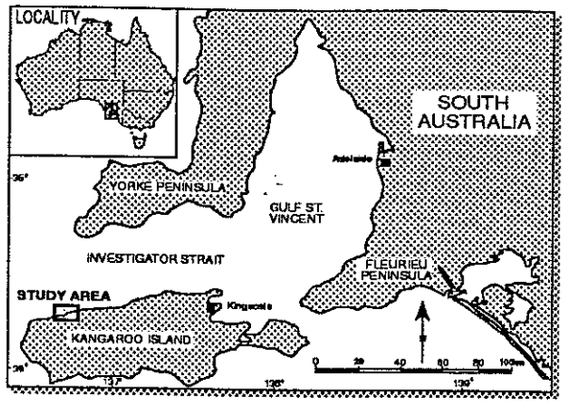

KEY TO MAP TWO

- BEDDING (S_0)
- OVERTURNED BEDDING (S_0)
- SEDIMENTARY YOUNGING DIRECTION
- CURRENT DIRECTIONS (unidirectional, bidirectional)
- TECTONIC BOUNDARY (thrust fault, strike slip fault)
- TRANSITIONAL LITHOLOGICAL BOUNDARY (observed/inferred)
- DOMINANTLY SHEARED ROCKS (1: porphyroblastic phyllonitic schist; 2: clean white quartz mylonite; 3: biotite-quartz mylonite; 4: quartz-biotite mylonite)
- **SEQUENCE ONE:** LAMINATED PSAMMITES & PELITES WITH MASSIVE MICACEOUS SANDSTONE AND GREYWACKE
- **SEQUENCE TWO:** MUDDY SANDSTONE & MEDIUM GRAIN GREY QUARTZITE, WITH PHYLLITIC PARTINGS

S_0 OUTSIDE SHEAR ZONE

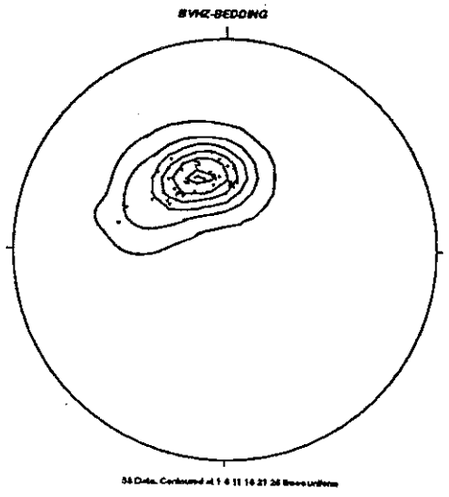

INVESTIGATOR STRAIT

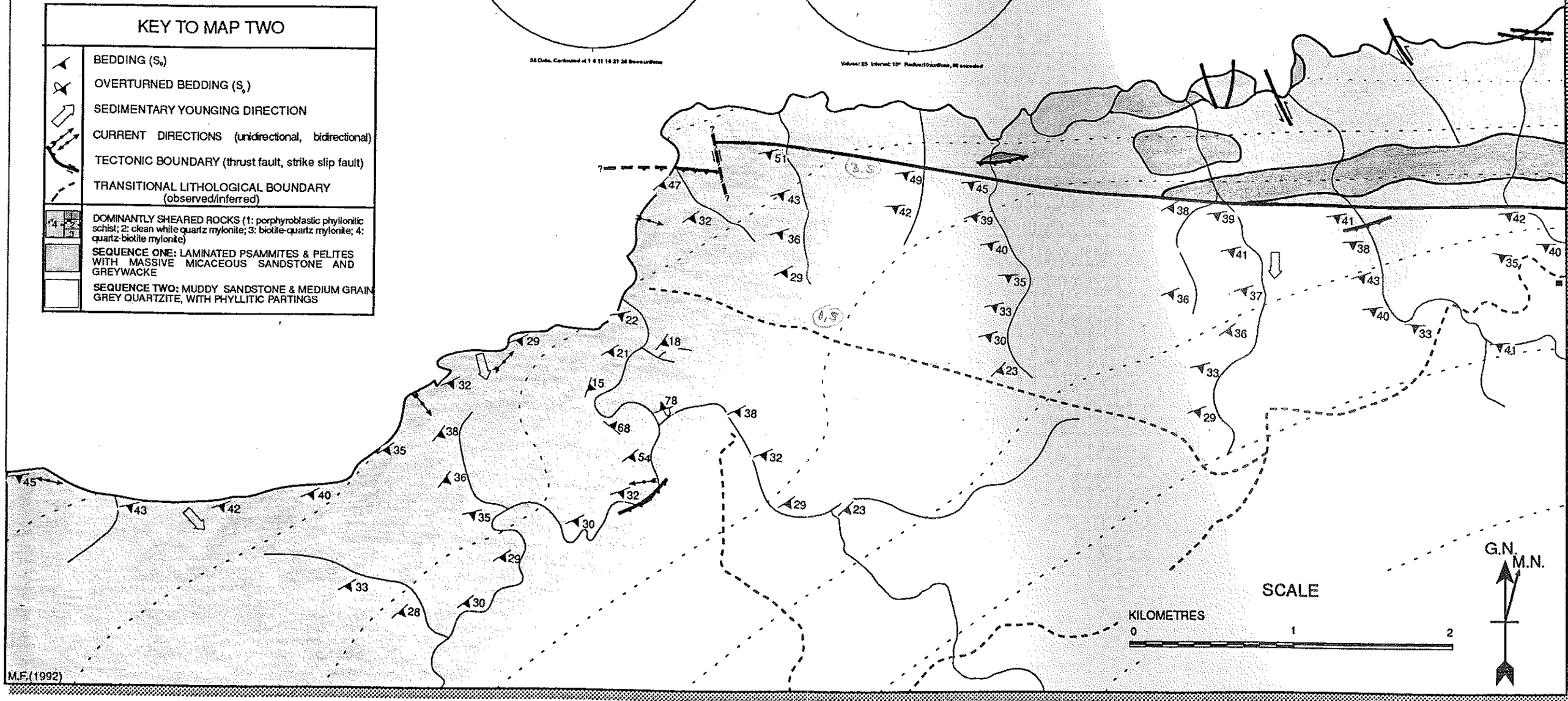

MAP THREE

GEOLOGY OF THE SNUG COVE-CAPE FORBIN AREA, KANGAROO ISLAND

SELECTED AXIAL PLANAR AND MYLONITIC FOLIATIONS, CRENULATION CLEAVAGES

KEY TO MAP THREE

	S_1 : SLATY CLEAVAGE/SCHISTOSITY, MYLONITIC FOLIATION IN SHEAR ZONE
	S_2: CRENULATION CLEAVAGE
3 2	DOMINANTLY SHEARED ROCKS (1: porphroblastic phyllonitic schist; 2: clean white quartz mylonite; 3: biotite-quartz mylonite)
	SEQUENCE ONE: laminated psammites and pelites with massive micaceous sandstone and 'greywacke'
	SEQUENCE TWO: Dirty sandstone and medium grained quartzite with phyllitic partings

SCSZ-CAPE FORBIN SUBDOMAIN-MYLONITIC FOLIATION

11 Data

SCSZ-MYLONITIC FOLIATION

32 Data Contoured at 1 3 5 9 13 17 21 Sigma Uniform

BVHZ-SLATY CLEAVAGE

31 Data contoured at 1 3 5 9 13 17 21 Sigma Uniform

SCALE

KILOMETRES

0 1 2

G.N. M.N.

MAP FOUR

GEOLOGY OF THE SNUG COVE-CAPE FORBIN AREA, KANGAROO ISLAND

SELECTED MINOR FOLD AXES, INTERSECTION LINEATIONS AND STRETCHING LINEATIONS

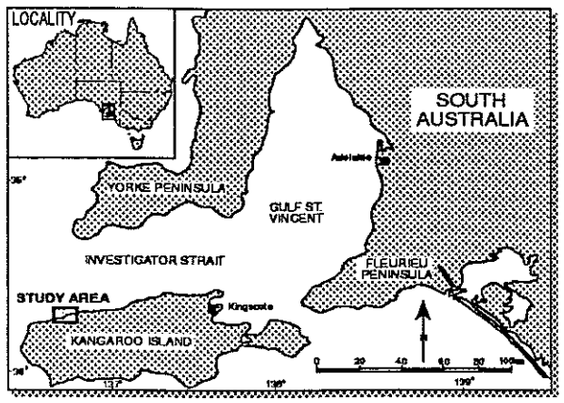

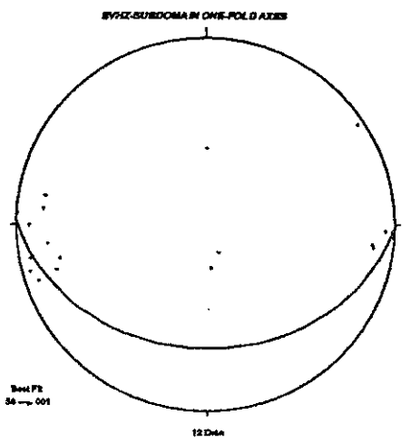

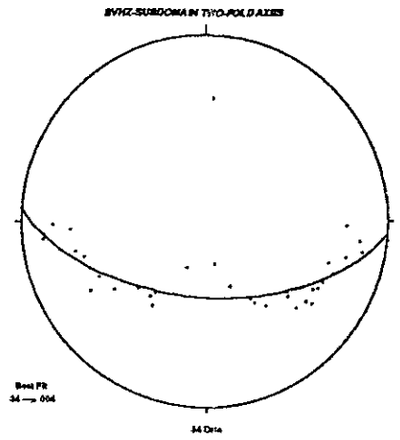

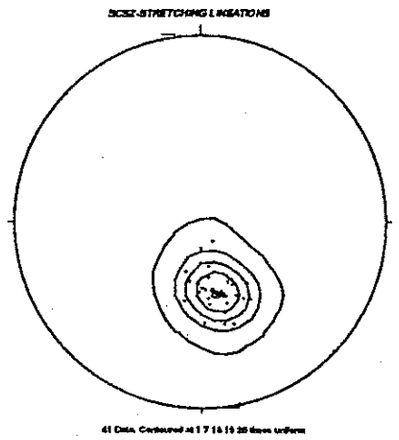

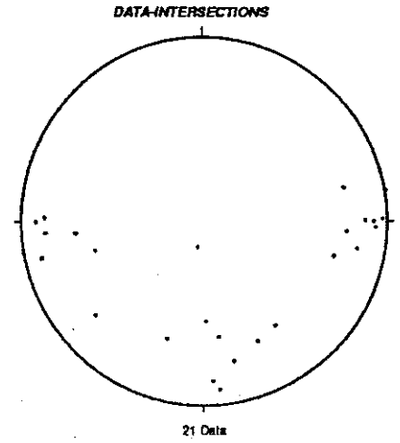

KEY TO MAP FOUR

- MINOR FOLD AXES (F_1)
- INTERSECTION LINEATIONS (L_1^s)
- STRETCHING LINEATIONS (L_1)
- TECTONIC BOUNDARY (thrust fault, strike slip fault)
- TRANSITIONAL LITHOLOGICAL BOUNDARY (observed/inferred)
- 3 2 DOMINANTLY SHEARED ROCKS (1: porphyroblastic phyllonitic schist; 2: clean white quartz mylonite; 3: biotite-quartz mylonite)
- **SEQUENCE ONE:** LAMINATED PSAMMITES & PELITES WITH MASSIVE MICACEOUS SANDSTONE AND GREYWACKE
- **SEQUENCE TWO:** MUDDY SANDSTONE & MEDIUM GRAIN GREY QUARTZITE, WITH PHYLLITIC PARTINGS

INVESTIGATOR STRAIT

SCALE

KILOMETRES 0 1 2

G.N. M.N.

M.F.(1992)

§3.2.1: Variation Of Fold Axial Planes And Interlimb Angles

Neglecting the effects of variation in fold styles (partly controlled by lithological factors), there is a clear transition from near upright to asymmetric overturned folds from south to north. Accompanying this change, the folds tighten and cleavage intensifies and rotates into slightly shallower orientations (Plate 2f). Fold interlimb angles range from *ca* 40°-150°, whilst associated local axial planar cleavage dips varied from *ca* 60°-40° to the south. The latter effect appears to be a separate feature from another common observed phenomenon; that of cleavage refraction across pelitic/psammitic interfaces. There is a distinct correlation between fold interlimb angle (FIA) and axial plane dip (APD), which was analysed statistically using a bivariate scatter diagram (Fig. 11). In order to minimise inaccuracies in FIA measurement, chevron-style folds were measured where possible.

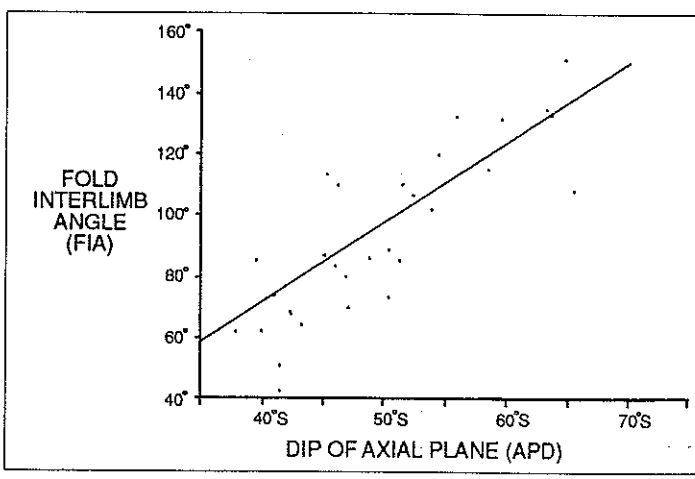

FIGURE 11: Bivariate scatter diagram showing correlation between Fold Interlimb Angle (FIA) and Axial Plane Dip (APD). The calculated correlation coefficient for this data is r = 0.79. The best fit linear regression line is also shown.

A model to account for the transition from near-upright to overturned folds must account for the rotation of axial planes and associated increase in strain magnitude (as indicated by tightening of the folds and cleavage intensification). Consequently a change in the orientation of the principle strain axes with increasing strain is proposed, ie a rotational strain. *Sanderson* (1980) has suggested such a mechanism, whereby sedimentary layers oriented at small angles to a shear plane respond to initial shortening along the layer by forming reasonably symmetric folds with axial planes at a high angle to the shear zone. Progressive simple shear produces a rotation of the fold axial planes towards parallelism with the shear plane and a tightening of the

folds due to further shortening. Figure 12 illustrates this concept with respect to the mapped geometry of the present study area.

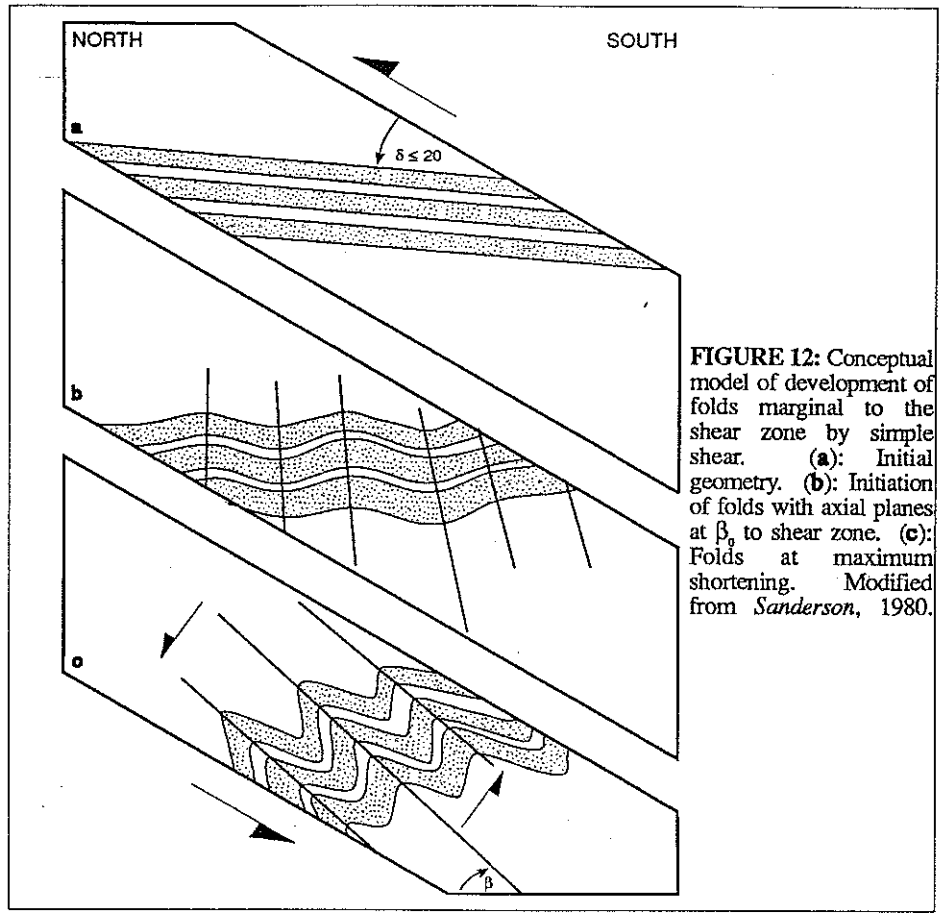

FIGURE 12: Conceptual model of development of folds marginal to the shear zone by simple shear. (**a**): Initial geometry. (**b**): Initiation of folds with axial planes at β_0 to shear zone. (**c**): Folds at maximum shortening. Modified from *Sanderson*, 1980.

By considering chevron folds only, *Sanderson* (1980) was able to approximate both the shortening values related to specific interlimb angles the magnitude of simple shear strain which caused the tightening and overturning of these folds. A significant proportion of folds within Sequence One deposits have high limb lengths relative to hinge curvature and thus approach chevron-style. A comparison of the results obtained by *Sanderson* (1980) with local interlimb angles and axial plane dips suggest that shortening values in the order of 20% are appropriate for near-upright open folds towards the southern (inland) limits of outcrop. Similarly, tight overturned folding in the vicinity of the Snug Cove Shear Zone provides semi-quantitative estimates of up to 50-60% shortening within individual folds. According to *Sanderson* (1980, figure 9) such values correspond to simple shear magnitudes ranging from $\gamma \ll 1$, up to $\gamma \approx 1$-3 proximal to the shear zone. These estimates can be regarded as minimum values only; additional post-buckle flattening is assessed in §3.2.2.

§3.2.2: Variation Of Fold Axis Orientations

Rare folds encountered towards the southernmost limits of inland outcrop were characterised by east-west sub-horizontal fold axes within steeply south dipping fold axial planes. However, outcrops elsewhere within the Back Valley Homoclinal Zone occasionally show abrupt and extreme variations in fold axis orientations, with occasional examples ofsub-horizontal folds occuring within several tens of metres of moderately and variably plunging folds. Where outcrop is continuous, the area between such folds is complexly deformed and often the site of a local decollement. The margins of the Snug Cove Shear Zone are host to both shallowly plunging and steeply plunging reclined fold axes. Within the shear zone, axes of isoclinal folds are subparallel to stretched quartz vein rods and a mineral stretching lineation. It is considered that the strain is essentially homogeneous on a mesoscopic scale and that heterogeneity is of a regional nature. Mesoscopic strain heterogeneity (multiple noncoaxial deformation) would be expected to lead to curved fold axes and/or cross-cutting axial planar fabrics indicative of overprinting deformations, neither of which is observed.

A similar spatial variation in fold axis orientation marginal to a shear zone has been recorded by *Bryant & Reed* (1969) adjacent to the Moine Thrust Zone, northwest Scotland. The origin of these reclined folds has been proposed by *Sanderson* (1973) to be due to the passive rotation of fold axes caused by stretching within the fold axial plane. Thus, with increasing strain ('stretching') in the XY-plane, folds originally sub-parallel to the Y-axis of the finite strain ellipsoid rotate towards the X-axis (ie the stretching lineation direction) upon further deformation. Furthermore, *Mancktelow* (1981) observed that local strain perturbations can account for the observed close proximity of subhorizontal and reclined folds. The dominantly passive behaviour of fold axes in the present study area is demonstrated by the relative lack of sheath folds in high strain regions (ie folds with curved fold hinges). *Sanderson* (1973) derived a theoretical basis for such rotation (Appendix Three) and demonstrated that the resulting 'post-rotation' frequency distribution of fold axes depends on:

1) the original variation (standard deviation, σ) in the orientation of fold axes, and

2) the ratio of the rotation-inducing principal strains (X/Y)

A series of graphs produced by *Sanderson* (op cit) shows computed frequency distribution of fold axis orientation with increasing X to Y ratio for differing original variabilities of the fold axes (Fig. 13a). Hence, a graphical evaluation of the state of strain indicated by fold axis distribution can be made. As can be seen by a comparison with these theoretical results, field data shows a slightly asymmetric frequency distribution. *Sanderson* (1973) suggested that such asymmetry can result from a slight obliquity between the mean fold axis and the Y-axis of the regional finite strain ellipsoid, and he accordingly produced theoretical distribution curves for a 10° difference between the two (Figure 13b).

Figure 13c shows that the actual distribution curve of the field data (of Subdomain Two) falls between curves for Y oriented parallel to the mean fold axis and Y at 10° to the mean fold axis. Therefore, it is suggested that fold axis orientations of the Back Valley Homoclinal Zone are consistent with average regional X/Y ratios of 2-3:1 with stretching at a high angle (but not perpendicular) to original fold axes. Such a feature is not unexpected, given that the stretching lineation in the XY-plane of higher strain zones is not perfectly downdip, but generally pitches ~80° within the foliation plane.(§3.3). In comparison fold axes from Subdomain One strike within 10° of east-west and thus record relatively low ratios of 0<X/Y<1.

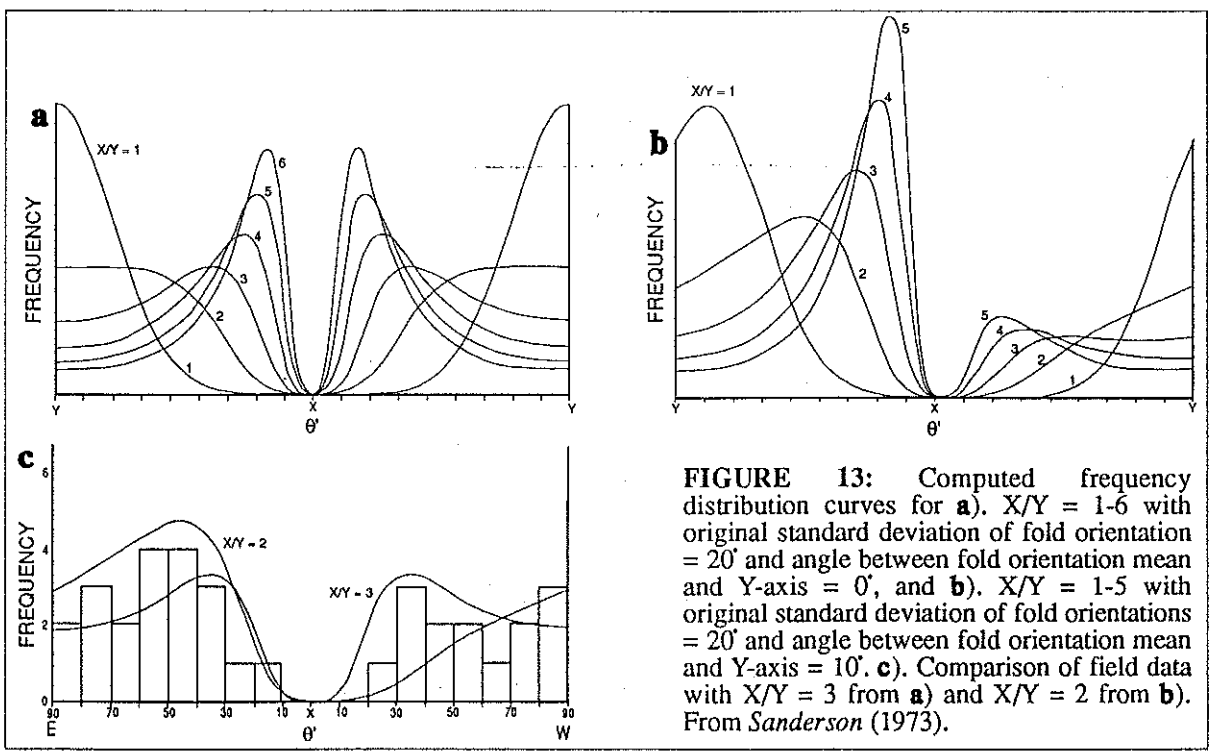

FIGURE 13: Computed frequency distribution curves for **a**). X/Y = 1-6 with original standard deviation of fold orientation = 20° and angle between fold orientation mean and Y-axis = 0°, and **b**). X/Y = 1-5 with original standard deviation of fold orientations = 20° and angle between fold orientation mean and Y-axis = 10°. **c**). Comparison of field data with X/Y = 3 from **a**) and X/Y = 2 from **b**). From *Sanderson* (1973).

§3.2.3: Fold Styles

Folds within Sequence One deposits were analysed in terms of *Ramsay's* (1967) fold classification scheme (Fig. 14) using field photographs and, more commonly, line drawings of photographs and actual outcrops.

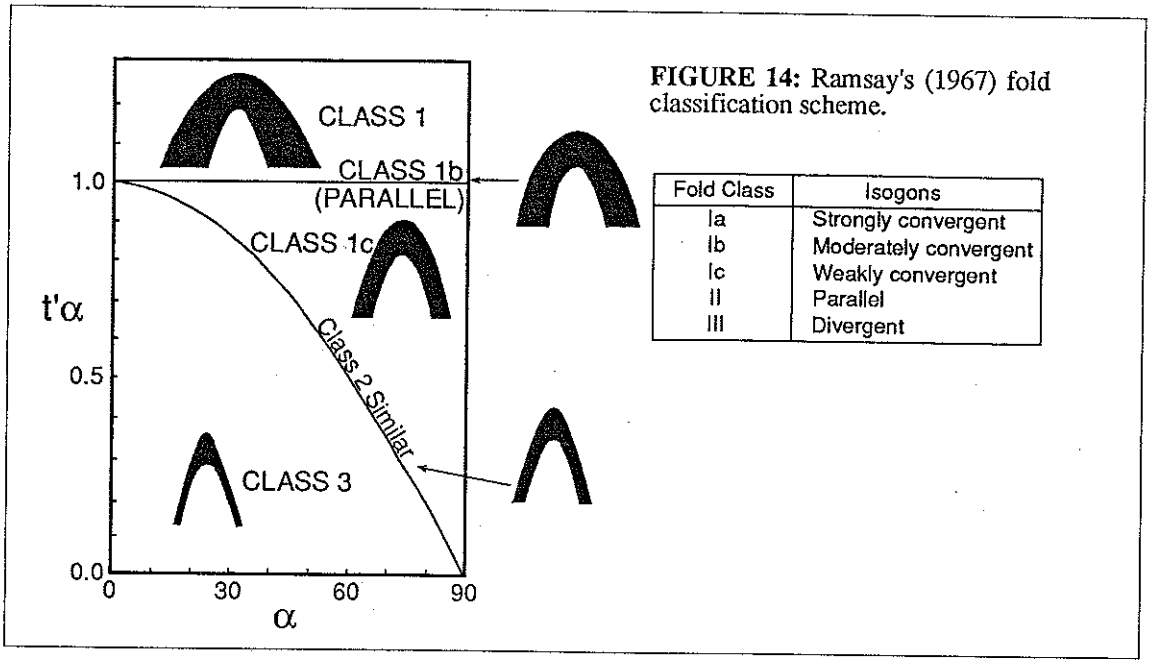

FIGURE 14: Ramsay's (1967) fold classification scheme.

Fold Class	Isogons
Ia	Strongly convergent
Ib	Moderately convergent
Ic	Weakly convergent
II	Parallel
III	Divergent

The style of folding observed *primarily* depended upon the scale of observation which in turn was related to lithology; ie. the gross alternation between laminated and non-laminated horizons, or within individual laminated multilayers. There is, of course, a continuous sequence between the two end-members (massive units grade into laminated units, and thick intermediate faintly laminated units are common). The lithological variation is defined largely by relative biotite concentrations of individual layers. For the purposes of structural analysis, the following distinction is made:

pelitic - abundant biotite

psammitic - sparse biotite

semi-pelitic - intermediate in biotite concentration (≈ pelitic/psammitic multilayers)

A fourth lithology, quartz veins, took the form of tight to ptygmatic Class Ic folds (if folded at all). Relatively thick psammitic layers were rarely observed to be folded. Instead, the

interface between the psammitic beds and pelitic multilayers was often observed to take the form of buckle-fold mullions (*Wilson*, 1953). In profile, the strong viscosity contrast between the two adjacent media has led to the development of lobes of more competent psammitic material seperated by cusps of tightly pinched less-competent, more pelitic, multilayer (Plate 3a). As is the case with the majority of folds in the study area, these mullions show moderate to strong asymmetry indicating northwards vergence. *Hudleston* (1973b) has demonstrated that, adjacent to the Moine Thrust Zone, such cuspate forms of pelitic multilayers are a consequence of the contact strain zone of adjacent more competent lithologies. Thus, in many cases, the fold styles of less competent horizons in the Cape Forbin area are merely a feature controlled by the fold style adopted by psammitic layers. In other examples, adjacent psammitic and pelitic horizons exhibited extremely disharmonic folding, with the latter being highly contorted in contrast to the relatively unaffected psammitic layer.

Multilayer units as a whole approached Class 2 fold styles (*Ramsay*, 1967), displaying near parallel dip isogons. Within multilayers, however, thin psammitic layers were found to have weakly convergent isogon patterns with adjacent pelitic layers exhibiting divergent isogons (Class 1c and 3 respectively of *Ramsay*, 1967). Semi-pelitic layers commonly displayed similar-style fold morphologies, with isogon paterns intermediate between psammitic and pelitic layers (ie Class 2 of *Ramsay*, 1967).

Hudleston (1973a) derived a procedure by which Class 1c folds can be used to estimate the amount of 'apparent' flattening strain required to produce such folds from buckle (Class 1b) folds. The method considers the angle between the normal to the folded surface isogons (ϕ) and the limb dip (α). A comparison of a graphical plot of $\alpha-\phi$ versus ϕ with mathematically derived curves enables the calculation of a specific relative Z/X ratio (from the slope of the best-fit line). Thus relative spatial variations in the intensity of finite flattening strain (X/Z ratios) can be determined.

In order to assess the strain magnitude variation from north to south across the study area 'Hudleston analyses' were conducted upon two populations of geographically seperated

Class 1b psammitic layers. Since quartz veins were largely Class 1c folds, thus displaying least post-buckle flattening, these were excluded from the analysis. In addition, the Hudleston technique makes no allowance for Class 3 pelitic folds, which were therefore similarly excluded. Estimates were averaged for several isolated folds at approximately 1000 and 100 metres from the mapped boundary of the Snug Cove Shear Zone (areas One and Two respectively). The results of this technique, together with examples of the folds utilised, are presented in Figure 14.

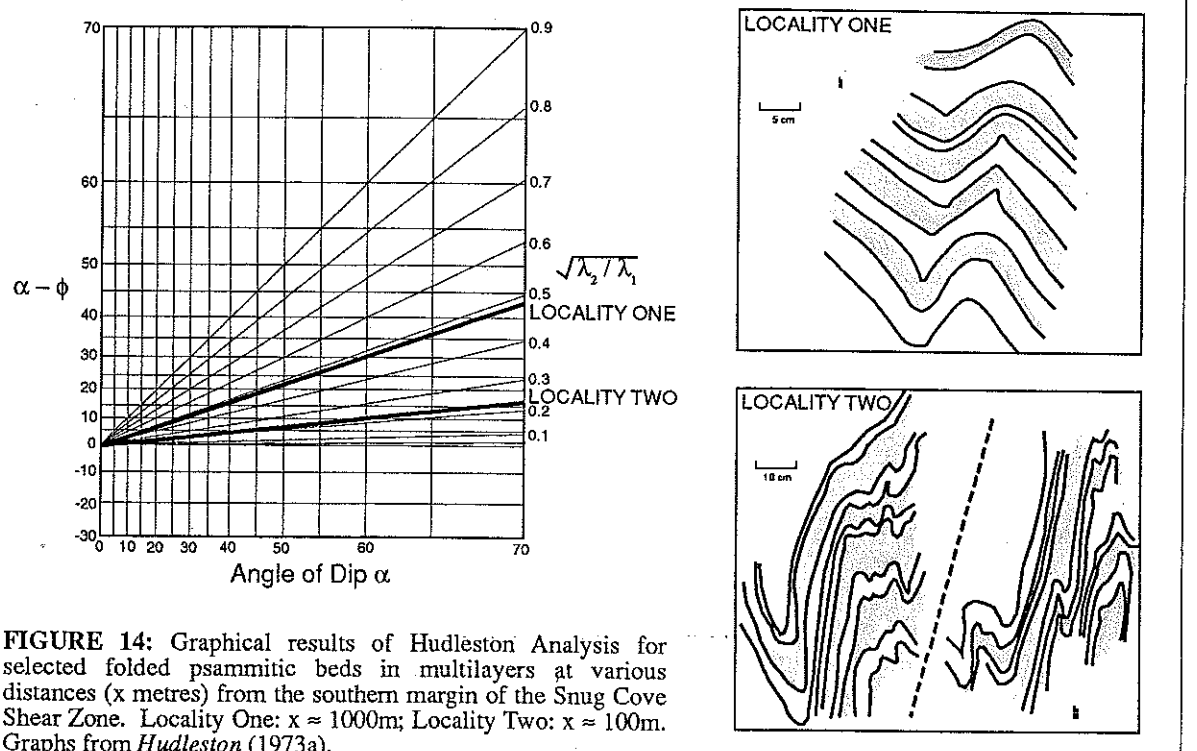

FIGURE 14: Graphical results of Hudleston Analysis for selected folded psammitic beds in multilayers at various distances (x metres) from the southern margin of the Snug Cove Shear Zone. Locality One: x ≈ 1000m; Locality Two: x ≈ 100m. Graphs from *Hudleston* (1973a).

Maximum and minimum X/Z flattening strains for Area One were 5.35:1 and 3.12:1 respectively, with an average value of 4.35:1. Similarly, estimates for Area Two ranged from 1.96:1 to 2.44:1, with a mean of X/Y = 2.08:1. These results, although relative estimates only, indicate quantitatively that finite 'post-buckle' flattening strains increase northwards, towards the Snug Cove Shear Zone.

§3.4: THE SNUG COVE SHEAR ZONE

Whilst the increase in strain intensity across the Back Valley Homoclinal zone is appreciable, a relatively rapid change marks the southern boundary of a zone of highly deformed rocks, the Snug Cove Shear Zone (Fig. 7). Several features delineate this transition. As has been noted, a tightening and overturning of folds is accompanied by a dramatic intensification of the regional schistosity and the appearance of a near down-dip stretching lineation. The foliation steepens (by as much as 10°) and acquires a phacoidal, mylonitic character. Originally planar quartz veins become buckled and/or flattened within the foliation plane and ultimately evolve into isolated quartz augens. The foliation anastomoses around these augens, producing an oyster-shell fluxion foliation (Plate 3b) characteristic of foliations formed by intense syn-tectonic recrystallisation during ductile non-coaxial shear (*James*, 1989a).

Folding of bedding and quartz veins was seen to become increasingly intense, producing highly attenuated fold limbs and, commonly, rootless intrafolial folds (Plate 3c). These folds are indicative of extreme flattening strains normal to the XY-plane of the local finite strain ellipsoid, produced by high simple shear strains. Moreover, fold axes in this high strain zone are sub-parallel to the pervasive stretching lineation, indicating X/Y ratios in excess of 5-6:1 (cf. Figure 13). Other quartz veins are highly boudinaged, rather than folded, depending upon whether they have rotated into the extensional component of the simple shear strain field. The asymmetry of these boudins suggests south over north shear (Plate 3d).

Disrupted lensoidal bedding, isoclinal folding, and the complete dominance of the mylonitic foliation in places ensures that the lithological layering within the Snug Cove Shear Zone has little or no stratigraphic significance. Indeed, one of the characteristic features of this structural domain is the failure of detailed mapping to establish anything but the crudest coherent lithological subdivision. Nevertheless, on a gross scale, three major lithostratigraphic units were recognised.

The majority of the outcrop within the Snug Cove Shear Zone comprises a massive biotite-rich quartz mylonite, superficially resembling Sequence One lithofacies (but more fine-grained and homogeneous). The eastern portion of the shear zone consists of both biotite-quartz mylonites and coarse-grained phyllonitic schists (with the previously described oyster-shell texture). The appearance of the latter muscovite-rich schists is coincident with the observation of andalusite and cordierite porphyroblastic horizons, and is presumably related to the more aluminous nature of argillaceous Sequence Two deposits towards the east of the study area. A third lithology, buff to white recrystallized quartzite, was mapped as discontinuous east-west trending macroscopic lenses, particularly comprising several coastal cliffs. The relationship between this unit and lithologies within the hangingwall of the shear zone is unclear.

It should be emphasised that lensoidal lithological layering occurs at all scales and that even gross stratigraphic variation across the shear zone can be attributed to such features. There is no evidence of appreciable discrete fault planes leading to thrust emplacement of lithologies, indeed east-west striking faults within the Snug Cove Shear Zone can be traced no more than several metres..

Macroscopic composite fabrics commonly associated with shear zones (ie. S-C fabrics) are not particularly well-developed within the Snug Cove Shear Zone, a feature possibly related to the homogeneity of biotite-rich quartz mylonites which dominate the area . Instead, much of the kinematic evidence for the shear zone comes from rotated quartz augen (Plate 3f), asymmetric boudins (Plate 3d) and microstructural evidence. Observations of the exposed shear zone boundary at Cape Forbin, combined with surface trace variation with topography, suggest that the Snug Cove Shear Zone dips moderately to the south at approximately 45°. The pervasive foliation consistently dips steeply to the south (~50-60°,Fig. 9), thus maintaining an angle of 5-15° relative to the shear plane, not the 45° expected of a mylonitic foliation at the margins of a shear zone in isotropic rocks. .Such a feature is probably related to the influence of a pre-existing sedimentary anisotropy (see §3.5).

§3.4: R_f/ϕ TECHNIQUE AND SUMMARY OF STRAIN ANALYSES

Various techniques of semi-quantitative and quantitative strain analysis have been outlined and utilized. The gradual tightening of folds proximal to the shear zone accompanied by a slight decrease in cleavage plane dip (§3.2.1) suggested that simple shear magnitudes ranging from $\gamma \ll 1$, up to $\gamma \approx 1\text{-}3$ are appropriate estimates in a south to north traverse across the Back Valley Homoclinal Zone. Hudlston analyses (§3.2.3) produced associated post-buckle apparent flattening strains across a similar area of X/Z = 2.08:1 and X/Z = 4.35:1 respectively. Rotation of fold axes within the XY-plane of the finite strain ellipsoid (§3.2.2) indicate a change in X/Y ratios across a similar traverse of X/Y = 1 to X/Y = 2-3. Fold axes subparallel to the stretching lineation similarly indicate X/Y > 5-6:1 within the margins of the Snug Cove Shear Zone (at least where folds in bedding are still distinguishable).

In order to further assess flattening strain across S_1, highly deformed early-syntectonic porphyroblasts and detrital quartz grains were used assess strain magnitude at two seperate localities. The porphyroblasts were from samples taken from the southern margin of the Snug Cove Shear Zone, whilst the quartz grains were analysed from thin-sections taken at ≈ 500m from this boundary, within the Back Valley Homoclinal Zone. XZ and YZ sections were used for both lithologies.

The R_f/ϕ technique, derived by *Hudleston* (1973a), relies upon the fact that a randomly oriented set of elliptical objects undergoing flattening will be distorted and rotated into a new orientation distribution (or 'fluctuation')with respect to a fixed reference line. Thus, the final object ellipticity (R_f) and fluctuation (f), is a function of the form (R_i) and orientation (ϕ) of the initial ellipse, and the form (R_s) and orientation (ϕ') of the local finite strain ellipse. Therefore the plot of R_f against ϕ' defines an array of points which can be compared with a computer derived curves for various strain magnitudes and initial ellipticities, giving quantitative estimates of the dimensions of the finite strain ellipsoid for both XZ and YZ planes. The method assumes only an initial random distibution and that the objects deform passively within their matrix. R_f/ϕ analysis was conducted using a digitising tablet to define the strain marker

dimensions as a series of points which were then analysed by the INSTRAIN computer program (*Erslev*, 1989) to produce appropriate scatterplots of the data. These results are presented in Figure 16.

The distribution of object ellipticities on the R_f /ø plot are reasonably symmetrical for both porphyroblasts and quartz grains, indicating an initial random distribution of orientations. A comparison of the scatterplots with the standard curves suggest that the porphyroblasts originally had no significant original ellipticity, suggesting that cleavage development had little effect upon the growth forms (a feature which was also observed in the shapes of the late-syntectonic andalusite porphyroblasts). In contrast, best fit curves for the quartz grain scatterplots suggest an appreciable original ellipticity was present. Given that the sample was taken from within the well-sorted and laminated Sequence One deposits, this is consistent with a pre-existing sedimentary fabric. The wide scatter of data points for quartz grain R_f /ø plots made the fitting of standard curves somewhat subjective, however, R_s values in the order of 1.5-2.0 are considered to be appropriate. Data for porphyroblasts, on the other hand enable confident estimates of $R_s = 3.5$ for the XZ-plane and $R_s = 1.5$ for the YZ-plane to be made. Thus, keeping in mind the locations of the samples used, results of R_f/ø analysis are consistent with other previously mentioned indications of increasing flattening strains to the north.

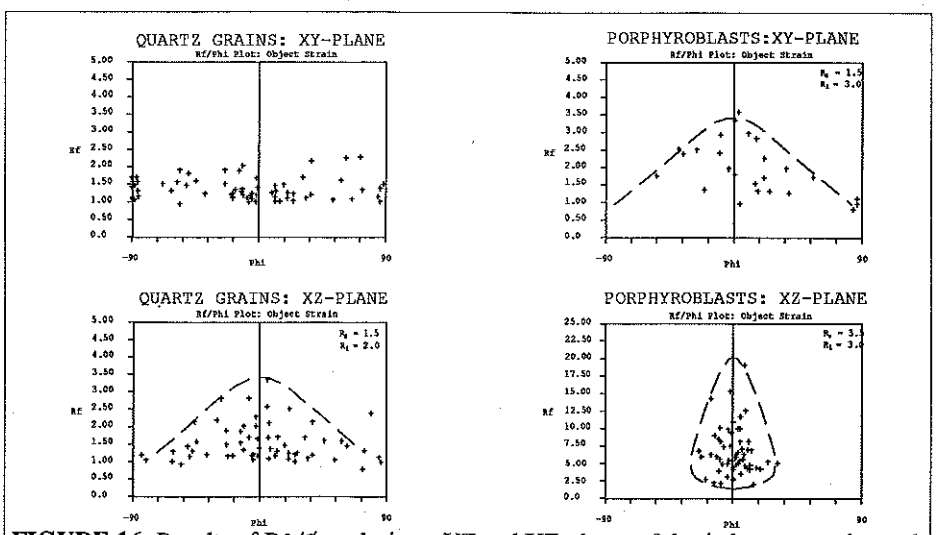

FIGURE 16: Results of Rf /ø analysis on YZ and XZ-planes of detrital quartz grains and retrogressed biotite-quartz porphyroblasts respectively. Quartz grains are from thin-sections taken ≈ 1000m from Snug Cove Shear Zone, porphyroblasts were located at the margins of the shear zone. Standard curves (from *Dunnet*, 1969) for specific R_S and R_i are shown for comparison.

§3.5: MICROSTRUCTURAL ANALYSIS

Twenty thin-sections were produced from samples obtained within the study area in order to determine mineralogical and microstructural variation accompanying mesoscopic changes. In many cases sections were produced for both XZ and YZ planes of the local finite strain ellipsoin, where maximum and minimum strain features respectively should be observed. Thin-sections A985-5a and A985-5b were used for R_f /ø analysis in §3.2.4 and contain relatively unrecrystallised detrital quartz grains. Sections A985-17a and A985-17b show microscopic views of highly flattened early to syntectonic porphyroblasts used in a comparative $R_f/ø$ analysis.

The lower strain Back Valley Homoclinal Zone thin-sections show minor elongation of quartz grains, with little apparent foliation defined by phyllosilicates (Subdomain One). Growth of metamorphic biotite had clearly not proceeded to any significant extent, because the majority of such grains exhibited no preferrred orientation, with some grains being truncated by sedimentary scours (and thus are clearly sedimentary - Section A985-17). Samples taken closer to the the shear zone (Subdomain Two) contain a distinct preferred alignment and recrystallisation of biotite defining S_1, with discordant concentrations of biotite delineating S_0, particularly in Sequence One deposits. More massive Sequence Two deposits show no appreciable foliation development in low strain zones. Rogers (1991) reported two discrete generations of metamorphic biotite in the Talisker area. No such distinction was apparent within the Cape Forbin area, although 'S_1' was commonly observed to be overegrown by late-stage muscovite and chlorite.

A northwards sampling traverse reveals that growth of metamorphic biotite increase, producing a more intense S_1 fabric. Quartz grains are noticably elongate, defining the stretching lineation, and grain boundaries show evidence of recrystallization (quartz overgrowths etc; *Knipe*, 1989). Recystallization is incomplete: detrital grains are still present. However, due to recrystallization, there has been a slight decrease in overall grain size (independent of starting composition since some sections were taken along to bedding strike).

Marginal to the Snug Cove Shear Zone, recrystallization of quartz grains dominates the thin-section fabric, along with pronounced phyllosilicate preferred orientation and growth. Bands of segregated mica are noticable, along with a distinct preferred crystallographic orientation of quartz grains. The majority of the rock appears to be comprised of fine-grain quartz crystals, a feature which *Knipe* (1989) has attributed to grain diminution by crytstal-plastic processes related to strain localization within shear zones.

Thin-sections taken from the same position relative to the shear zone margin, but towards the east, show two distinct populations of porphyrblasts. A highly deformed set of retrogressed biotite-quartz porphyroblasts clearly predate a significant majority of the deformation, and thus record a large component of the strain history (§3.4). A relatively undeformed set of andalusite porphyroblasts appear to be late to syntectonic. These porphyroblasts occasionally show inclusion trails, the majority of which show apparent rotation indicating south-over-north shear. However, because of the equivocal nature of these sense-of-shear indicators (some show contradicting senses of rotation on opposite sides of the same object), other forms of kinematic indicators were utilized. Quartz augens and asymmetric pressure shadows (*Passchier & Simpson*, 1986) on both microscopic and mesoscopic scales (Plate 3e) indicate top-to-the-north shear in approximately 65-70% of cases, as do displacement of microfractures along the S_1 foliation.

Samples from the most internal parts of the Snug Cove Shear Zone show almost complete recrystallization of quartz and biotite grains. Sections taken along lithological strike into the western portions of the shear zone show progressive quartz grainsize diminution, culminating in section A985-5, which exhibits a fine-grained groundmass of highly elongate grains. Sections from the eastern half of the shear zone show extensive phyllosilicate growth anastomosing around quartx augen, presumably reflecting the argillaceous nature of Sequence Two deposits in the hangingwall of this area. These sections are taken from the phyllonitic schists shown in Plate 3b. Grain diminution of quartz (Plate 3), extensive mica growth and marked pressure shadow development are all consistent with increasing strain to the north.

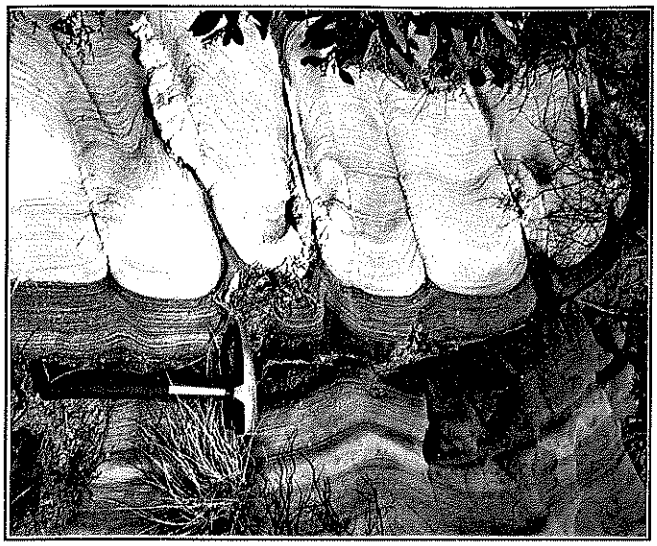

PLATE 3a: Fold mullions. Note hammer for scale. View looking east. [Snug Cove; 589452].

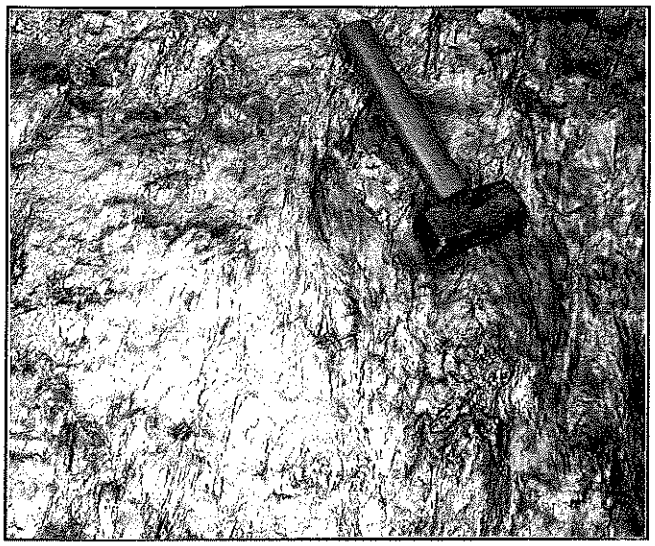

PLATE 3b: 'Oyster-shell' texture produced by quartz augens in a phyllonitic schist. Note mallet for scale. View of XY-plane. [Snug Cove; 639478].

PLATE 3c: Rootless intrafolial folding of quartz veins, YZ-plane. Width of view ≈ 60 cm. [Snug Cove; 619478].

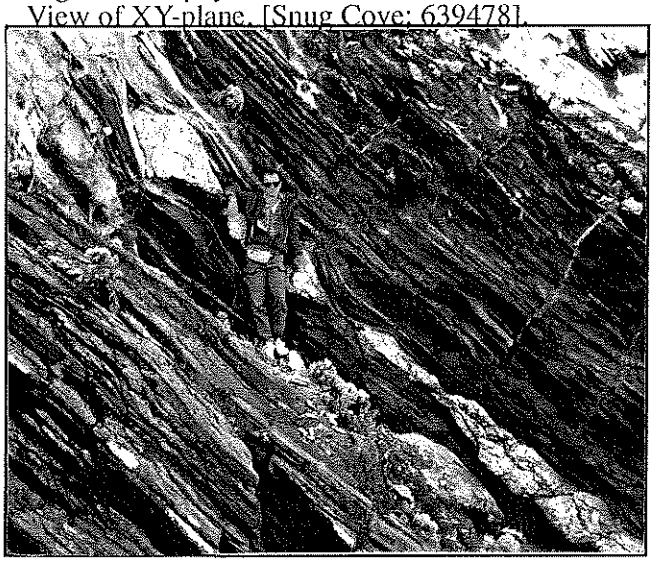

PLATE 3d: Large-scale asymmetric boudins indicating top-to-north shear. Note figure for scale. View to east. [Snug Cove;611475].

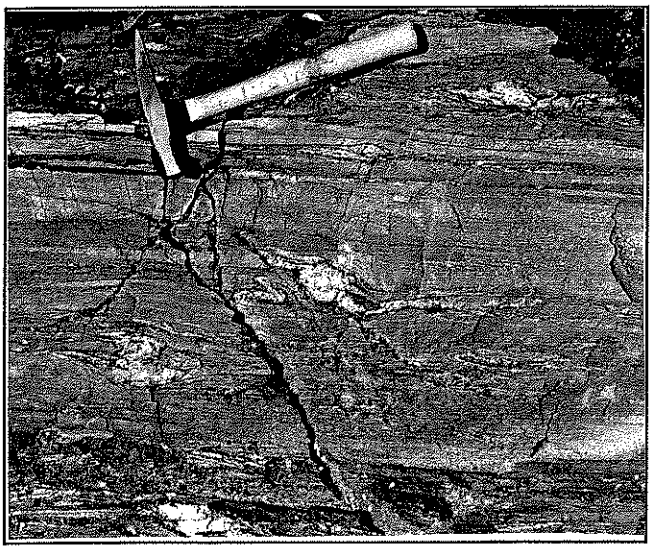

PLATE 3e: Rotated mesoscopic quartz augen indicating top-to-the-north simple shear. Note hammer for scale. [Snug Cove; 641478].

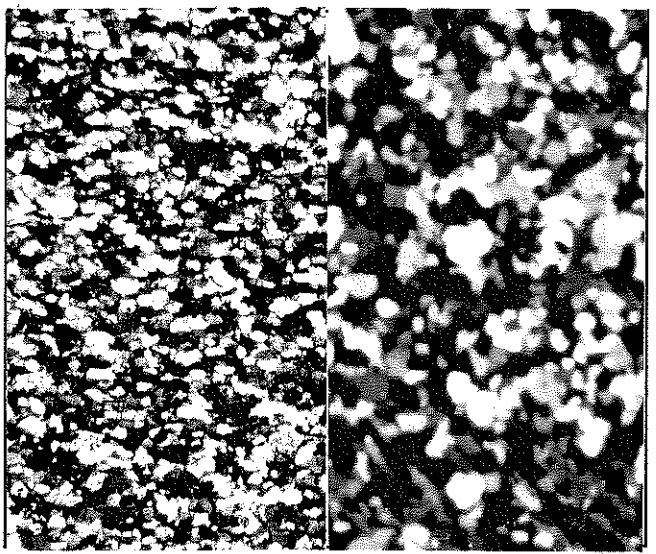

PLATE 3f: Composite microphotograph illustrating progressive grainsize diminution. Width of view ≈ 5mm.

§4: REGIONAL SIGNIFICANCE, SYNTHESIS AND CONCLUSIONS

The lower, northernmost boundary of the Snug Cove Shear Zone was not observed within the study area (but is predicted to crop out further east, Fig. 3). However geophysical data provides valuable constraints upon unexposed portions of the shear zone. Recent gravity and magnetic profile modelling (*Van der Stelt et al*, 1992), combined with offshore sample dredging has provided a reinterpretation of the geometry of the Gawler Craton to the north of Kangaroo Island (*Belperio & Flint*, 1992a). Details of these studies reveal that, locally at least, the Snug Cove Shear Zone is coincident with the southern limits of Lincoln Complex gneissic basement at shallow depths (Fig. 17). Thus it is entirely likely that the boundary between probable Tapanappa Formation equivalents and Palaeoproterozoic basement in the Cape Forbin area is the zone of highly sheared Kanmantoo Group rocks mapped in this study.

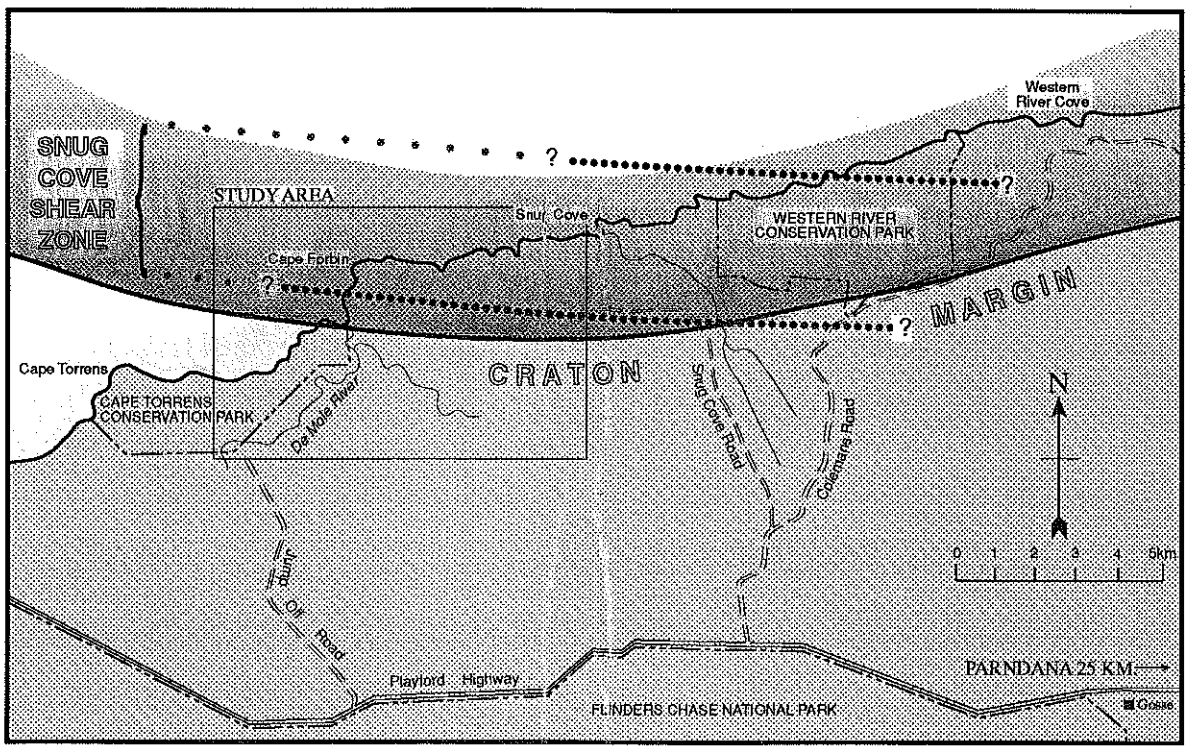

FIGURE 17: Regional relationship between the interpreted southern margin of the Gawler Craton and the Snug Cove Shear zone. Note that the location of the northern edge of the shear zone is poorly constrained by field evidence. Data from this study and *McCallum* (1991).

A structural model of the Cape Forbin area must account for the observed spatial variation in structural styles and strain intensity. Qualititative estimates of strain magnitude are in agreement with qualititative observations of increasing strain intensity northwards,

culminating in extreme strain localization within the Snug Cove Shear Zone. Simple shear mechanisms can account for much of this variation. *Sanderson* (1979) has suggested that such variation is attributable to the spatial transition from the 'supra-structure' to 'infra-structure' within a thrusted terrain.

Gray & Willman (1991) point out that thrust sheet mechanical behaviour and emplacement shows a spectrum between rigid and viscous gliding models. The latter requiring displacement by ductile yield in the hanging wall which is reflected by penetrative deformation of the sheet, particularly towards the base. Extreme localisation of ductile deformation at the base of thrust sheets can occur (*Gray & Willman*, 1991). Moreover, fold geometry, cleavage intensity, lineation development and total strain magnitude vary with structural position within iNdividual thrust-sheets. These features are thus consistent with the geology of the Cape Forbin area. Therefore the current erosion level of the study area is interpreted to represent a section through progressively deeper portions of a single thrust-sheet, culminating in the Snug Cove Shear Zone.

Gray & Willman (1991) derived a strain profile through a typical thrust-sheet within the Ballarat Slate Belt, with a similar geometry to that described from the Cape Forbin area. *Rogers* (1991) demonstrated that such a strain profile was applicable to the (ductile) Coalinga Creek Shear Zone in the Talisker area. This typical strain profile is shown in Figure 18.

The strain data outlined in §3 and the presence of the ductile Snug Cove Shear Zone suggest that, in the classification of *Gray & Willman* (1991), the Cape Forbin area represents a section through Domains II and III of the typical thrust sheet. In this respect the shear may thus represent the basal decollement below the thrust sheet. Given that a significant portion of the lower Kanmantoo Group and the Adelaide Supergroup are apparently not present in the Cape Forbin area (Fig. 2), then either these lithologies were not deposited in the region or that significant tectonic transport has occured across the shear zone. Given the thickness of Kanmantoo lithologies elsewhere on Kangaroo Island and the great vertical extent of the shear zone (indicating appreciable displacement), the latter option is most likely.

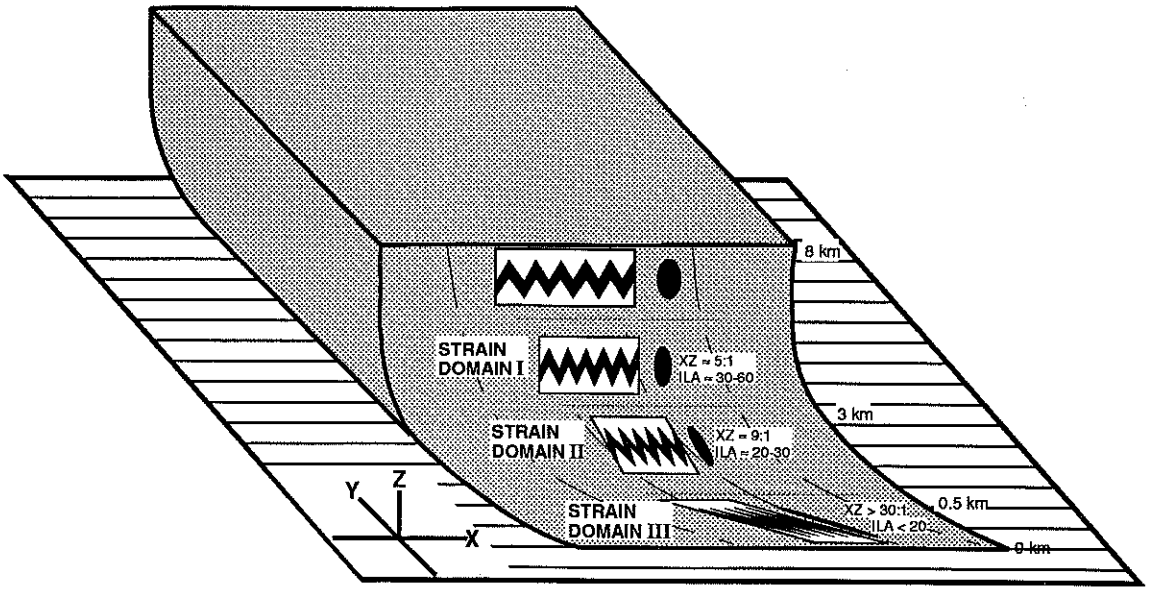

FIGURE 18: Thrust-sheet model showing strain profile through a typical thrust-sheet from the Ballarat Slate Belt. The thrust-sheet is seperated into strain domains based upon strain magnitudes and fold geometries with different distances from the basal decollement. Modified from *Gray & Willman* (1991) and *Sanderson* (1982).

Intuitively, the presence of a marked mechanical anisotropy would play a significant role in focussing deformation and localizing strain within a fault or shear zone (however, see *Sandiford* et al, 1992, concerning the effects of thermal perturbation). Furthermore, with the presence of north-verging structural criteria outlined previously, one would expect an appreciable component of 'buttressing' of the sedimentary pile against the rigid Gawler Craton, a feature proposed to account for strain localization in other foreland fold-thrust belts. Such buttressing effects produce extreme flattening within the deforming rocks. Although simple shear mechanisms are evident within the Cape Forbin area, a significant component of synchronous pure shear flattening can not be discounted. Indeed it provides an alternative explanation for the high flattening strains as indicated by strain markers, the lack of variation in the orientation of the mylonitic foliation in the shear zone, the absence of well-developed S-C fabrics and the relatively low proportion of unequivocal microscopic kinematic indicators. If the foliation is partly a result of pure homogeneous flattening then the possibility remains that it's orientation is, in part, a consequence of the geometry of the craton margin. Strain factorization into pure shear and simple shear is not possible with such limited strain data, but it is suggested that a significant component of thrust sheet shortening via flattening is present in the Cape Forbin area, a feature common in other thrust sheets elsewhere (*Sanderson*, 1982).

The present study has raised several problems which may provide a focus for future studies. On Dudley Peninsula (Fig. 3),*Menpes* (in prep.) has reports the presence of narrow zones of dominantly strike-slip deformation seperated by large near dip-slip domains., and has proposed a model involving regional-scale transpression to account for such observations. However, similar areas of sub-horizontal stretching lineations were not recognised in the Cape Forbin area. Instead, tectonic transport directions were consistently oblique to near down-dip throughout the area. Further detailed local work is required to explain this discrepancy, and to ascertain the role of transpressional mechanisms along the Snug Cove-Point Morrison Shear Zone system. In addition, a further problem remain with respect to the regional significance of the shear zone. Whilst locally the Snug Cove Shear zone is the likely contact zone between Archaean/lower Proterozoic basement and Palaeozoic cover rocks, to the east Kanmantoo Group equivalents occur *to the north* of the probable trace of the shear zone (Fig. 3). Consequently, structural complications at depth must be invoked to explain the variation in structural position and significance of this major zone of relatively intense deformation. Therefore subsequent structural investigations should ideally be concentrated upon the structurally lowermost margins of the Snug Cove Shear Zone, which is anticipated to crop-out several kilometres to the west of Western River Cove (Fig. 3).

The proposed structural model for the present study area has important implications for the regional geology of the southern Adelaide Fold Belt. Inherent in the 'thrust-sheet' concept is that some displacement of the hangingwall block has occurred, which can account for the present tectonic juxtaposition of Kanmantoo Group over and against basement rocks. Relative movement between the upper and lower boundaries of the thrust sheet may exceed 1-2 kilometres. Whilst the Snug Cove Shear Zone is not a classic brittle thrust-fault encountered in typical fold-thrust belts, the tectonic translation resulting may be similar, albeit at deeper crustal levels. This type of sheared contact with basement rocks is not uncommon within the Adelaide Fold Belt (James, 1989a) and has been used to support models of significant structural detachment. Thus the structural geometry within the present study area is consistent with the current reinterpretation of the orogen as the 'southern Adelaide Fold-Thrust Belt'.

Firstly and foremost, I would like to acknowledge the guidance provided by my illustrious leaders, Drs. Pat James and Thomas Flöttmann, and the role they played in shaping the final thesis. Just as important were my 'Claytons' supervisors; Drs. Richard Jenkins and Mike Sandiford for helpful discussions throughout the year (particularly the latter, for intellectual stimulation by argument!). In addition I would like to acknowledge Dr. Steve ('The Guru') Marshak for the American perspective, and for providing simple and clear explanations to complex concepts - the man should be writing textbooks.

Thanks are also extended to the incredibly varied and interesting bunch of Kangaroo Islanders who helped make two months of fieldwork an unforgettable experience; Haydn & Marg Wilkinson and family for hospitality above and beyond the call of geology; Graham Burnett for the hi-octane home brew and the conversations that followed ("rocks!...what rocks?"); 'Ceefa the possum' and his countless proteges for many a sleepless night and after-dark exercise; a multitude of friendly Islanders whom I briefly socialised with. The South Australian Department of Mines and Energy are (particularly Tony Belperio) are thanked for logistical and equipment support, that enabled some of this mayhem.

Furthermore, I wish to thank many members (and ex-members) of the Department:

- the Honours class of 1992, for keeping me amused and sane throughout the year (particularly the 'structure boys' - Rob ('Possum Poker') Menpes, Marc Twining, Pasquale ('Subaru Killer') Cesare and Jerome ('Gemini Killer') Randabel. Let's not forget psuedo-structure girl Tricia Farrow, who showed me how to really slam Tequilas),
- Garry Adams, for much helpful criticism of my thesis (and much sledging of me). Ditto Simon Wetherly (University of Western Australia) and Adam Crossing ('Croffing'?),
- Gary Ferris, for reading of seemingly endless drafts, and using his 'been-there-done-that' knowledge for my benefit (particularly with regards to some potential pitfalls),
- various members of the 1992 3rd Year class and 'Sparky' Hillis, for some very eventful trips.

Mostly, I wish to thank my entire family for support throughout my Undergraduate and Postgraduate years, especially my parents (you know who you are - I hope!). Hopefully the multitude of late-night meals, grumpy moods and endless costs will be worthwhile.....

REFERENCES

Bauer, F.H., (1958). The regional geography of Kangaroo Island, South Australia. Ph.D. thesis, Australian National University (unpublished).

Belperio, A.P. & Flint, R.B., (1992a). The geological and geological framework of Kangaroo Island. *South Australia. Department of Mines and Energy. Report Book, 92/1.*

Belperio, A.P. & Flint, R.B., (1992b). The southern margin of the Gawler Craton. *Australian Journal of Earth Sciences*, **39**, in press.

Boord, R.A., (1985). Sedimentation of the Cambrian, upper Kanmantoo Group, southern Fleurieu Peninsula, South Australia. B.Sc.(Hons.) thesis, University of Adelaide (unpublished).

Bryant, B. & Reed, J.C., (1969). Significance of lineation and minor folds near major thrust faults in the southern Appalachians and the British and Norwegian Caledonides. *Geological Magazine*, **106**, 412-429.

Clarke, G.L. & Powell, R., (1989). Basement-cover interaction in the Adelaide Foldbelt, South Australia: the development of an arcuate foldbelt. *In* Ord, A. (ed.), Deformation of Crustal Rocks. *Tectonophysics*, **158**, 209-226.

Daily, B. & Milnes, A.R., (1971a). Stratigraphic notes on Lower Cambrian fossiliferous metasediments between Campbell Creek and Tunkalilla Beach in the type section of the Kanmantoo Group, Fleurieu Peninsula, South Australia. *Transactions of the Royal Society of South Australia*, **95**, 199-214.

Daily, B. & Milnes, A.R., (1971b). Discovery of Late Precambrian tillites (Sturt Group) and younger metasediments (Marino Group) on Dudley Peninsula, Kangaroo Island, South Australia. *Search*, **2**, 431-433.

Daily, B. & Milnes, A.R., (1972). Significance of basal Cambrian metasediments of andalusite grade, Dudley Peninsula, Kangaroo Island, South Australia. *Search*, **3**, 89-90.

Daily, B. & Milnes, A.R., (1973). Stratigraphy, structure, and metamorphism of the Kanmantoo Group (Cambrian) in it's type section east of Tunkalilla Beach, South Australia. *Transactions of the Royal Society of South Australia*, **97**, 213-242.

Daily, B., Milnes, A.R., Twidale, C.R. & Bourne, J.A., (1979). Geology and Geomorphology. *In:* Tylor, M.J., Twidale, C.R. & Ling, J.K. (eds.), Natural History of Kangaroo Island. *Royal Society of South Australia. Occasional Publications*, 3, 1-38.

Daily, B., Moore, P.S., & Rust, B.R., (1980). Terrestrial-marine transition in the Cambrian rocks of Kangaroo Island, South Australia. *Sedimentology*, **27**, 379-399.

Dunnet, D., (1969). A technique of finite strain analysis using elliptical particles. *Tectonophysics*, **7**, 117-136.

Erslev, E., (1989). INSTRAIN - an integrated analysis program for the Macintosh. *Rockware Inc.*

Fenton, M.W., & Wilson, C.J.L., (1985). Shallow-water turbidites: an example from the Mallacoota Beds, Australia. *Sedimentary Geology*, **45**, 231-260.

Flint, D.J., (1978). Deep sea fan sedimentation of the Kanmantoo Group, Kangaroo Island. *Transactions of the Royal Society of South Australia*, **102**, 203-222.

Flint, D.J. & Grady, A.E., (1979). Structural geology of Kanmantoo Group metasediments between West Bay and Breakneck River, Kangaroo Island. *Transactions of the Royal Society of South Australia*, **103**, 45-56.

Flöttmann, T. & James, P.R., (1992). Tectonic evolution of the southern Adelaide Fold Belt: a strain and balanced-section approach. *Geological Society of Australia. Abstracts* **32**, 241.

Flöttmann, T., James, P.R., Johnson, T. & Rogers, J., (1992). Fault and shear zone minor- and micro-structures and fabrics associated with large scale thrusting in the Talisker area of the southern Fleurieu Peninsula, South Australia. *Geological Society of Australia. Abstracts* **32**, 231-232.

Foden, J.D., Turner, S.P., Sandiford, M., Williams, I., Compston, W. & Michard, A., (1992). The Nature, Timing and Duration of the Delamerian-Ross Orogeny. *Journal of the Geological Society*. in press.

Gatehouse, C.G., Jago, J.B. & Cooper, B.J., (1990). Sedimentology and stratigraphy of the Carrickalinga Head Formation (low stand fan to high stand systems tract), Kanmantoo Group, South Australia. *In:* Jago, J.B. & Moore, P.S. (eds.), The evolution of a Late Cambrian-Early Palaeozoic rift complex: the Adelaide Geosyncline. *Geological Society of Australia. Special Publication,* **16**, 351-366.

Gravestock, D.I., (in prep.). Cambrian. *In*: Johns, R.K. (ed.), The geology of South Australia. *South Australia. Geological Survey. Bulletin, 54.*

Gray, D.R., & Willman, C.E., (1991). Thrust-related strain gradients and thrusting mechanisms in a chevron-folded sequence, southeastern Australia. *Journal of Structural Geology, 13*, 691-710.

Hudleston, P.J., (1973a). Fold morphology and some geometrical implications of theories of fold development. *Tectonophysics*, **16**, 1-46.

Hudleston, P.J., (1973b). The analysis and interpretation of minor folds developed in the Moine rocks of Monar, Scotland. *Tectonophysics*, **17**, 89-132.

Hudleston, P.J., (1989). The association of folds and veins in shear zones. *Journal of Structural Geology*, **11**, 949-957.

James, P.R., (1989a). Field Excursion Guide - Structural geology of the Fleurieu Peninsula. *Specialist Group in Tectonics and Structural Geology. Conference Field Guide.*

James, P.R., (1989b). Field Excursion Guide - Structural geology of Kangaroo Island. *Specialist Group in Tectonics and Structural Geology. Conference Field Guide.*

Jenkins, R.J.F., (1986). Ralph Tates enigma - and the regional significance of thrust faulting in the Mt. Lofty Ranges. *Geological Society of Australia, Abstracts*, **15**, 101.

Jenkins, R.J.F., (1990). The Adelaide Fold Belt: Tectonic reappraisal. *In:* Jago, J.B. & Moore, P.S. (eds.), The evolution of a Late Cambrian-Early Palaeozoic rift complex: the Adelaide Geosyncline. *Geological Society of Australia. Special Publication,* **16**, 396-420.

Jenkins, R.J.F. & Sandiford, M., (1992). Observations on the tectonic evolution of the southern Adelaide Fold Belt. *Tectonophysics*, **214**, in press.

Johnson, T.M., (1991). The structure of the Blowhole Creek area, southern Adelaide Fold Belt, Fleurieu Peninsula, South Australia. B.Sc.(Hons) thesis, University of Adelaide (unpublished)

Knipe, R.J., (1989). Deformation mechanisms - recognition from natural tectonites. *Journal of Structural Geology*, **11**, 127-146.

Major, R.B. & Vitols, V., (1973). The Geology of the Vennachar and Borda 1:50,000 Map Areas, Kangaroo Island. *Mineral Resources Review, South Australia*, **134**, 38-51.

Maltman, A., (1981). Primary bedding-parallel fabrics in structural geology. *Journal of the Geological Society of London*, **138**, 475-483.

Mancktelow, N.S., (1979). The structure and metamorphism of the southern Adelaide Fold Belt. Ph.D. thesis, University of Adelaide (unpublished).

Mancktelow, N.S., (1981). Variation in fold axis geometry and slaty cleavage microfabric associated with a major fold arc, Fleurieu Peninsula, South Australia. *Journal of the Geological Society of Australia*, **28**, 1-12.

Mancktelow, N.S., (1990). The structure of the southern Adelaide Fold Belt. *In:* Jago, J.B. & Moore, P.S. (eds.), The evolution of a Late Cambrian-Early Palaeozoic rift complex: the Adelaide Geosyncline. *Geological Society of Australia. Special Publication,* **16**, 369-395.

McCallum, W.S., (1991). Geological investigations and drilling, Parndana area, Kangaroo Island 1989-1990. *South Australia. Department of Mines and Energy. Report Book, 91/23.*

Offler, R. & Fleming, P.D., (1968). A synthesis of folding and metamorphism in the Mt Lofty Ranges, South Australia. *Journal of the Geological Society of Australia*, **15**, 245-266.

Owen, G., (1987). Deformation processes in unconsolidated sands. *In*: Jones, M.E. & Preston, R.M.F. (eds.), Deformation of Sediments and Sedimentary Rocks. *Geological Society Special Publication*, **29**, 11-24.

Passchier, C.W. & Simpson, C., (1986). Porphyroclast systems as kinematic indicators. *Journal of Structural Geology*, **8**, 831-834.

Preiss, W.V., (1987). The Adelaide Geosyncline. Late Proterozoic stratigraphy, sedimentation, palaeontology and tectonics. *South Australia. Geological Survey. Bulletin, 53*.

Price, N.J., & Cosgrove, J.W., (1990). *Analysis of geological structures*. Cambridge University Press. Cambridge.

Ramsay, J.G., (1967). *Folding and fracturing of rocks*. McGraw-Hill. New York.

Reading, H.G., (1986). *Sedimentary Environments and Facies*. Second Edition. Blackwell Scientific Publications Oxford. .

Rogers, J., (1991). The structure of the Talisker area, southern Adelaide Fold Belt, Fleurieu Peninsula, South Australia. B.Sc.(Hons.) thesis, University of Adelaide (unpublished).

Sandiford, M., Foden, J., Zhou, S. & Turner S., (1992). Granite genesis and the mechanics of convergent orogenic belts with applications to the southern Adelaide Fold Belt. *Proceedings of the Royal Society of Edinburgh: Earth Sciences (Second Hutton Symposium),* **83**, 83-93.

Sanderson, D.J., (1973). The development of fold axes oblique to the regional trend. *Tectonophysics*, **16**, 55-70.

Sanderson, D.J., (1980). The transition from upright to recumbent folding in the Variscan fold belt of southwest England: a model based on the kinematics of simple shear. *Journal of Structural Geology*, **1**, 171-180.

Sanderson, D.J., (1982). Models of strain variation in nappes and thrust sheets: a review. *Tectonophysics*, **88**, 201-233.

SADME, (1990). Southern margin of the Gawler Craton. *South Australia. Department of Mines and Energy. Mineral Industry Quarterly,* **57**, 3-4.

Sprigg, R.C., Campana, B. & King, D., (1954). KINGSCOTE map sheet. *South Australia. Geological Survey. Geological Atlas 1:253 000 Series,* sheet SH53-5

Sprigg, R.C. & Campana, B., (1953). The age and facies of the Kanmantoo Group, eastern Mt Lofty Ranges and Kangaroo Island, South Australia. *Australian Journal of Science*, **16**, 12-14.

Steinhardt, C., (1989). Thrusting and the tectonic evolution of the Adelaide Geosyncline. *Geological Society of Australia, Abstracts*, **24**, 140.

Talbot, J.L. & Hobbs, B.E., (1968). The relationship of metamorphic differentiation to other structural features at three localities. *Journal of Geology*, **76**, 581-587.

Thomson, B.P., (1969). The Kanmantoo Group and Early Palaeozoic tectonics. *In* Parkin, L.W. (ed.), *Handbook of South Australian Geology.*, 97-108. Government Printer, Adelaide.

Thomson, B.P., (1975). Kanmantoo Trough -regional geology and comments on mineralisation. *In:* Knight, C.L., (ed.), *Economic Geology of Australia and Papua New Guinea, Vol. 1 Metals.* The Australasian Institute of Mining and Metallurgy, Melbourne, p. 560-565.

Turner, S.P., Foden, J.D., Sandiford, M. & Bruce, D., (1992). Sm-Nd isotopic evidence for the provenance of sediments from the Adelaide Fold Belt and southeastern Australia with implications for crustal growth models. in press.

Van der Stelt, B., Belperio, A.P. & Flint, R.B., (1992). Geophysical appraisal of northern Kangaroo Island. *South Australia. Department of Mines and Energy. Report Book, 92/2.*

Wilson, G., (1953). Mullion and rodding structures in the Moine Series of Scotland. *Proceedings of the Geological Association*, **64**, 118-151.

Wood, D.S., (1974). Current views on the development of slaty cleavage. *Rev. Earth Planet. Sci., 2*, 369-401.

SANDERSON TECHNIQUE

Consider a population of fold axes, or bedding/cleavage intersection lineations, normally distributed about a mean. If the mean orientation of the fold axes is parallel to the Y-axis of the finite strain ellipsoid, the fold axes will be subject to a stretching normal to their mean direction. Through progressive deformation the fold axes will both rotate and change in length. These factors will influence the frequency distribution of the fold axes. The problem of rotation is essentially a two-dimensional one as β lies within the XY-plane of the strain ellipsoid. The change in length of β is considered relative to the length of Y and hence the relative lengths of axes will be independent of Z and whether the finite strain ellipsoid is prolate or oblate.

A Gaussian distribution for local Y strain axes as a function of θ, $Y_{(\theta)}$, yields a frequency distribution function (**D.F.**):

$$Y_{(\theta)} = \left(\frac{N}{\sigma\sqrt{2\pi}}\right)^{-\frac{1}{2}\left(\frac{90-\theta}{\sigma}\right)^2} \qquad (1)$$

where: N = population size

σ = standard deviation from the mean

θ = angle between the fold axes and the X strain axes

With further (e.g. progressive) deformation, producing a stretching in X, fold axes will be rotated towards X by the transformation:

$$\tan\theta = X/Y \tan\theta' \qquad (2)$$

where: X/Y = ratio of principal axes of the strain ellipsoid in the XY-plane

θ' = transformed value of Y

From equation (2):

$$\theta' = \tan^{-1}(Y/X\tan\theta) \qquad (3a)$$

$$\theta = \tan^{-1}(X/Y\tan\theta') \qquad (3b)$$

In addition, the length of fold axes will also change, also effecting the probability of them being sampled. Consequently this will effect the resulting distribution. The change in line length is given by the quadratic elongation, λ:

$$\lambda = \lambda_1\cos^2\theta + \lambda_2\sin^2\theta \qquad (4)$$

By dividing (4) by λ_2 and, since $\lambda_1/\lambda_2 = (X/Y)^2$, we get:

$$\lambda_1/\lambda_2 = (X/Y)^2\cos^2\theta + \sin^2\theta$$

If all lengths are considered relative to Y, we derive the sampling factor (**S.F.**):

$$\boxed{\text{S.F.} = [(X/Y)^2\cos^2\theta + \sin^2\theta]^{\frac{1}{2}}} \qquad (5)$$

If we consider an original distribution made up of grouped data with a constant class interval, then after deformation these class intervals will change and will no longer be of a constant size. The rate of change of some small interval $\delta\theta'$ with respect to $\delta\theta$ can be found by differentiating equation (3a):

$$\theta' = \tan^{-1}(Y/X\tan\theta)$$

$$\delta\theta' = \frac{X/Y}{(X/Y)^2\cos^2\theta + \sin^2\theta}\,\delta\theta$$

The deformed frequency distribution involves division of the original distribution by a class interval function in order to normalise the frequency distribution. Consequently we can define a class-interval function (**C.I.F.**):

$$\boxed{\text{C.I.F.} = \frac{X/Y}{(X/Y)^2\cos^2\theta + \sin^2\theta}} \qquad (6)$$

Combining the original distribution function, D.F. (1), the class-interval function, C.I.F. (6) and the sampling function, we get an expression for the new frequency distribution of the deformed data in terms of $\theta(Y_0)$:

$$\boxed{Y_{(\theta)} = \frac{\text{D.F. x S.F.}}{\text{C.I.F.}} = \left(\frac{N}{\sigma\sqrt{2\pi}}\right)^{-\frac{1}{2}\left(\frac{90-\theta}{\sigma}\right)^2} \frac{[(X/Y)^2\cos^2\theta + \sin^2\theta]^2}{X/Y}} \qquad (7)$$

HUDLESTON TECHNIQUE (based on Hudleston, 1973)

This technique can only be performed on the profile planes of class I(c) folds (see *Ramsay*, 1967; Figure 9), and assumes that the folds were initially class I(b) (parallel), folds before undergoing a bulk homogeneous flattening strain. It is this flattening strain that transforms the original I(b) fold into its final I(c) configuration.

Phi (ϕ) is defined as the angle between the normal to the tangent down to either fold surface, at the angle of apparent dip (α) , and the isogon. Values of $\alpha-\phi$ versus α are then plotted on a graph, which are compared to precalculated curves to derive an 'apparent' strain ratio $(\lambda 2/\lambda 1)^{1/2}$. However, because this ratio may not be a true measure of the strain accommodated by a natural fold, Hudleston refers to this value as an 'apparent' strain value. The method can, however, be used to determine the relative variation of the magnitude of the 'true' finite strain for each fold. Once the 'apparent' strain has been calculated, the principle quadratic elongations$\{(\lambda 1)^{1/2}$ & $(\lambda 2)^{1/2}\}$ can be deduced and their magnitudes compared for each fold. The technique was conducted on class I(c) folds in all three structural zones, and can be compared with results obtained by the Rf/ϕ analysis.

Figure 22

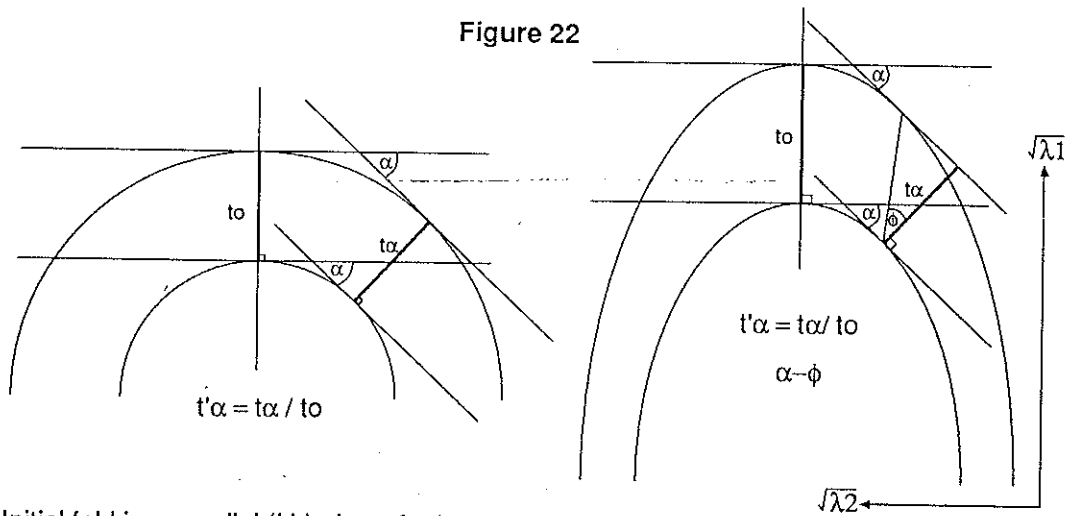

Initial fold is a parallel (I b) class, further strain transforms the original I(b) fold into its final I(c) configuration. $\sqrt{\lambda 1}$ and $\sqrt{\lambda 2}$ are the principle quadratic elongations, produced by the apparent strain ratio.

SUMMARY OF THIN SECTION DESCRIPTIONS

NOTE:

1) Thin-sections have prefix "TS" followed by sample number from which section was taken and the corresponding orientation with respect to the local finite strain ellipsoid, if applicable.

2) Thin-sections and corresponding hand specimens are located in the collection of the Department of Geology & Geophysics, University of Adelaide, accession number A985.

TS-A985-4a-XZ: phylonitic schist displaying phyllosilicate seams anastomosing around intensely isoclinally folded and disrupted quartz augens (Snug Cove Shear Zone).

TS-A985-4b-YZ: as for previous section, but in a plane of lower strain.

TS-A985-5a-XZ: quartz-biotite phyllite/schist showing partial recrystallisation and elongation of quartz grains and distinct preferred orientation of phyllosilicates. Note post-cleavage muscovite and chlorite.

TS-A985-5b-YZ: as for previous section, but in a plane of lower strain.

TS-A985-6: quartz mylonite showing intense recrystallisation of quartz grains and a strong, spaced pressure solution cleavage (or shear bands?).

TS-A985-7: sedimentary contact between reworked quartz-biotite laminae and poorly sorted, immature greywacke, showing a sedimentary scour structure. Note the apparent truncation of a large primary biotite grain (not mimectic) by the scour, in contrast to the preferentially aligned metamorphic biotite.

TS-A985-8-XZ: profile section of intensely developed axial planar cleavage defined by preferred crystallographic orientation of biotite. Bedding is nearly orthogonal to cleavage.

TS-A985-9-XZ: quartz vein at higjh angle to bedding, showing median line indication a possible tensional origin.

TS-A985-10-XZ: Sequence One laminated psammite/pelite showing strong S_0 with only weakly developed S_1 and no significant quartz elongation.

TS-A985-11-XZ: intensely deformed and recrystallised phyllonitic schist and quartz veinlet. Snug Cove Shear Zone.

TS-A985-12-XZ: section through axial planar quartz vein showing intrustion into small-scale fold hinge. Note bedding at high angle to vein margin.

TS-A985-16aXZ: mylonitic quartz-biotite schist with extremely flattened porphyroblasts (up to 10:1 aspect ratios). Porphyroblasts have retrogressed to biotite cores with quartz rims. Margins of Snug Cove Shear Zone.

TS-A985-16b-YZ: as for previous section, but in a plane of lower strain.

TS-A985-19a-XZ: biotitic quartzite with slightly flattened porphyroblasts (<2:1 aspect ratios). Porphyroblasts have retrogressed to biotite cores with quartz rims. Back Valley Homoclinal Zone.

TS-A985-19b-YZ: as for previous section, but in a plane of lower strain.

TS-A985-21-XZ: quartz-biotite schist with mylonitic foliation defined by strongly elongate quartz grains and growth of metamorphic biotite. Snug Cove Shear Zone.

TS-A985-22-YZ: large thin-section showing flattened, early-syntectonic retrogressed porphyroblasts and late syntectonic andalusite porphyroblasts.

TS-A985-24-YZ: moderately deformed biotitic quartzite with flattened quartz grains and partial growth of metamorphic biotite.

TS-A985-25-XZ: microfracures in biotitic quartzite shown by offset of bedding.

TS-A985-26-XZ: large section showing anastomosing mylonitic foliation wrapping around late-syntectonic andalusite poikyloblasts. Note contradictory shear sense indicators. (SCSZ).

SUMMARY OF FIELD PHOTOGRAPHIC DESCRIPTIONS

NOTE:

1) Locations of photograph views, including plates used within the main text, are given as geographic grid co-ordinates for South Australian Department of Lands 1:50 000 topographic sheets. "SC" = Snug Cove sheet, "B" = Borda sheet.

2) All originals of slide negatives are kept with Dr. T. Flöttmann, Department of Geology & Geophysics, University of Adelaide.

SLIDE 1: (*SC602463*); tabular cross-stratification within Sequence One deposits

SLIDE 2: (*SC609464*); erosional scour profile with greywacke overlying laminated Sequence One

SLIDE 3: (*B573451*); folded psammite/pelite multilayer of Sequence One deposits

SLIDE 4: (*SC593454*); liquefaction of greywacke and Sequence One multilayer

SLIDE 5: (*SC588452*); large-scale crossbedded channel sands within Sequence One deposits

SLIDE 6: as for slide 5

SLIDE 7: as for slide 2

SLIDE 8: (*SC609464*); turbiditic trough cross-laminations grading into reworked flat-laminations

SLIDE 10: (*B579452*); overturned minor fold with south dipping axial planar cleavage

SLIDE 11: (*SC608464*); tectonically modified ?sedimentary structures within Sequence One deposits

SLIDE 12: (*SC609464*); T_C part of Bouma Sequence with reworked flat-laminated top

SLIDE 13: (*B471426*); lobe-and-cusp structure within psammitic layer with axial planar quartz veins

SLIDE 14: (*SC611475*); asymmetric large-scale boudinage of quartz vein, Snug Cove Shear Zone

SLIDE 16: (*SC588451*); cross-bedding, Sequence One deposits

SLIDE 17: (*B482427*); highly flattened fold defined by quartz vein

SLIDE 19: as for slide 14

SLIDE 20: (*SC665467*); stepped slickenfibres on quartz veins

SLIDE 21: (*SC665475*); offset of quartz veins across sheared phyllitic beds, Sequence Two deposits

SLIDE 22: (*SC590452*); preferential quartz vein development in psammite layers,Sequence One

SLIDE 23: (*B579451*); folding around quartz veins

SLIDE 24: (*B578451*); bedding parallel slip causing offset of south dipping quartz veins

SLIDE 25: (*SC621477*); intense disruption of quartz veins, Snug Cove Shear Zone

SLIDE 26: (*SC654471*); andalusite porphyroblasts showing bedding plane control of growth

SLIDE 28: as for slide 8

SLIDE 29: (*SC611472*); relatively undeformed rocks thrust over Snug Cove Shear Zone rocks

SLIDE 30: (*B472425*); lobe-and-cusp structures with associated quartz veining

SLIDE 31: as for slide 30

SLIDE 32: as for slide 26

SLIDE 33: (*B573452*); tabular cross-laminations, Sequence One deposits

SLIDE 34: (*SC644477*); folded first and second order folds in quartz vein, Snug Cove Shear Zone

SLIDE 35: (*SC665470*); shearing preferentially confined to phyllitic horizons

SLIDE 36: (*SC624477*); intensely disrupted quartz veins (YZ-plane), Snug Cove Shear Zone

SLIDE 37: (*SC650478*); isoclinal folding, Snug Cove Shear Zone

SLIDE 38: as for slide 14

SLIDE 39: (*SC631475*); sigmoidal en echelon tension gashes, Snug Cove Shear Zone

SLIDE 40: (*SC665483*); refolded, transposed bedding, Snug Cove Shear Zone

SLIDE 41 as for slide 40

SLIDE 42: (*SC649478*); intrafolial, isoclinal folding, Snug Cove Shear Zone

SLIDE 43: (*SC611472*); faulted contact of shear zone and homoclinal zone (to right)

SLIDE 44: (*SC611472*); unsheared rocks faulted over sheared rocks (note disrupted quartz veins,)

SLIDE 45: (*SC645478*); oblique-dip stretching lineation in recrystallised quartzite, shear zone

SLIDE 46: (*SC643477*); oyster-shell texture (muscovite around disrupted quartz augens), shear zone

SLIDE 47: (*SC609465*); cuspate folding, Sequence One deposits

SLIDE 48: (*SC632477*); rootless intrafolial folding within intense ductile flow fabric, shear zone

SLIDE 49: (*B563452*); asymmetric mullions

SLIDE 50: as for slide 47

SLIDE 51: (*SC590452*); disharmonic, intrafolial folding, Sequence One deposits